Journal of
Polymer Materials

Tech Science Press

https://doi.org/10.32604/jpm.2026.077807

REVIEW

Recent Advances in Nanocellulose-Based Aerogels: Fabrication, Functionalization and Applications

Lin Jia and Qiang He*

College of Mechanical Engineering, Jiamusi University, Jiamusi, China

*Corresponding Author: Qiang He. Email: heqiang4532@163.com

Received: 17 December 2025; Accepted: 09 March 2026; Published: 03 April 2026

ABSTRACT: Aerogels, renowned as ultra-lightweight solids with exceptional porosity and specific surface area, have emerged as pivotal materials for thermal insulation, catalysis, energy storage, and biomedicine. This review comprehensively evaluates the recent strides in sustainable, high-performance cellulose-based aerogels, emphasizing their fabrication, functionalization, and application prospects. It details the extraction of cellulose from diverse sources and its subsequent processing into nanocellulose (e.g., cellulose nanofibrils and nanocrystals), which serves as the fundamental building block for aerogel synthesis. The critical sol-gel transition, solvent selection, and the pivotal role of drying techniques—freeze-drying, supercritical drying, and ambient pressure drying—in determining final aerogel architecture and properties are systematically analyzed. Special emphasis is placed on the advanced chemical modification of nanocellulose, including esterification, click chemistry, etherification, silanization, and amidation, which tailors surface chemistry to impart hydrophobicity, reactivity, or specific binding sites. The profound influence of cellulose source characteristics (aspect ratio, crystallinity, surface charge) on the pore-forming mechanism and aerogel performance is thoroughly discussed, bridging raw material selection with microstructure design. The review further elucidates the engineering of hybrid and composite aerogels by integrating silica, graphene, polymers, semiconductors, and metal-organic frameworks (MOFs), which synergistically enhance functionalities for targeted applications such as adsorption, photocatalysis, energy storage, sensing, and biomedical engineering. Despite significant progress, challenges remain in scalable green fabrication, balancing ultra-high porosity with mechanical robustness, and deepening the mechanistic understanding in complex applications. This work consolidates the current state-of-the-art, identifies key knowledge gaps, and provides a forward-looking perspective on the development of cellulose aerogels as versatile platforms for next-generation sustainable technologies.

KEYWORDS: Nanocellulose; aerogels; functionalization; nanocellulose-based composites; drying methods; hybrid materials

1 Introduction

Aerogels, recognized as among the lightest solid materials, are typically synthesized from organic, inorganic, or hybrid molecular precursors via a sol–gel process followed by specialized drying techniques. These materials possess a three-dimensional porous architecture that bridges nanoscale and larger pores, thereby retaining the intrinsic physicochemical properties of their precursors while endowing them with characteristic advantages of porous solids, such as high porosity, large specific surface area, ultra-low density, and extremely low thermal conductivity. Owing to these attributes, aerogels have found broad utility as thermal insulators, adsorbents, catalyst carriers, energy-storage media, and biomedical scaffolds [1–3]. In particular, their high specific surface area provides abundant active sites and enhances the contact probability

between catalysts and reactants, which effectively promotes catalytic efficiency. Consequently, aerogels have attracted considerable interest as promising heterogeneous catalytic materials.

Two principal strategies are employed for fabricating aerogel-based catalysts: the direct synthesis from molecular precursors and the self-assembly approach. The former involves the condensation and hydrolysis of molecular precursors (e.g., alkoxysilanes or metal alkoxides) to form gel networks, a method widely used for SiO_2 aerogels and applicable to certain metal-oxide aerogels (e.g., TiO_2, Al_2O_3, ZrO_2) [4–6]. Aerogels produced via this route generally exhibit relatively low crystallinity. In contrast, the self-assembly strategy, which often employs pre-formed nanoscale building blocks, yields aerogels with higher crystallinity and has been successfully extended to metal sulfides, metal oxides, and even metal-free systems. Moreover, the self-assembly approach offers greater versatility for designing composite aerogels that incorporate diverse catalytic components [7–9]. Regardless of the strategy, the aerogel preparation process fundamentally comprises two critical stages: the sol-to-gel transition and the subsequent gel-to-aerogel conversion.

The choice of solvent is very important in the process of sol nanoparticle formation. Taking silica aerogel as an example, the precursor is first dissolved in solvent, hydrolysis or alcoholysis occurs, and then silane reagent is added to complete the preparation process. In the preparation process, the solvent selected must have the ability to dissolve the substrate and form a homogeneous mixture [10]. Common solvents include ethanol, methanol, acetone, and tetrahydrofuran. As shown in Fig. 1, the three-phase diagram of silane-water-ethanol shows that when ethanol is used as a solvent, it has a good solubility to the substrate and will reduce the hydrolysis rate in the esterification reaction. When the solvent is unable to dissolve the silane reagent, it will lead to the aggregation of nanoparticles [11].

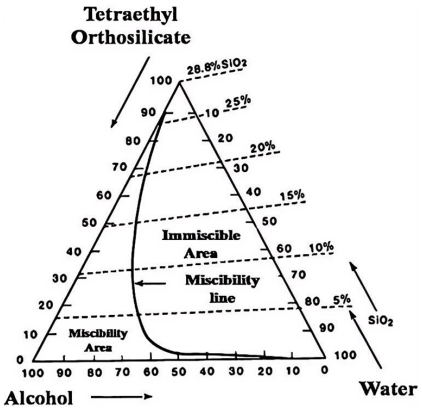

Figure 1: Three phase diagram of silane-water-ethanol [11]. Copyright © 2015 American Chemical Society.

At transition from sol to gel stage, the sol molecules themselves cross-link to form a three-dimensional frame structure, and then form a stable gel state. In the process of gel formation, it is generally necessary to evenly stir for 5 to 6 h to achieve its own crosslinking. During the crosslinking process, the stability of the gel can be changed by adjusting the temperature, pressure or pH value. In addition, the stirring rate and reaction temperature have significant effects on the shape and structural properties of the gel [12,13].

In the process of sol conversion to aerogel, water and ethanol in the pores need to be replaced into gas by a specific drying process means, in which the regulation of process conditions is crucial to maintain a complete 3D pore structure. In the process of solvent removal and drying, if the pore structure collapses, the physical and chemical properties of the aerogel will be directly reduced [14]. Therefore, in the process of sol conversion into aerogel, the regulation of drying parameters plays a very important role in the structure of aerogel [15,16].

The choice of drying method is equally critical, as it directly determines the pore architecture, mechanical integrity, and economic viability of the final aerogel [17,18]. Common techniques include freeze-drying (lyophilization), supercritical drying (typically using CO_2), and ambient pressure drying. Freeze-drying preserves the pore structure by sublimating the frozen solvent, but ice crystal growth can introduce microcracks and larger pores, affecting mechanical uniformity. Supercritical drying, which avoids liquid–gas interfaces by surpassing the solvent's critical point, yields aerogels with minimal shrinkage and high specific surface area, but requires expensive high-pressure equipment and rigorous safety protocols [19]. Ambient pressure drying is the most cost-effective and scalable option, yet it often necessitates prior solvent exchange to low-surface-tension liquids (e.g., tert-butanol) and/or surface modification to reduce capillary forces that cause pore collapse [20]. A comparative analysis of these methods-considering pore stability, processing cost, energy consumption, and suitability for specific applications-is therefore essential for guiding the scalable production of high-performance nanocellulose aerogels.

This review aims to provide a comprehensive and critical analysis of recent advances in cellulose-based aerogels, with a distinctive focus on bridging the gap between fundamental material engineering and application-driven design. Unlike prior reviews that often segment discussions on synthesis, modification, or applications, this work presents an integrated narrative that traces the evolution of cellulose aerogels from raw material selection through tailored chemical and physical functionalization to the rational fabrication of hybrid and composite architectures. We explicitly address the underexplored yet critical influence of cellulose source on final aerogel properties-a key variable for reproducible and scalable performance. Furthermore, by systematically categorizing and comparing hybridization strategies with silica, graphene, polymers, semiconductors, and metal-organic frameworks (MOFs), this review elucidates structure-property-application relationships. This approach not only consolidates the current state-of-the-art but also identifies precise knowledge gaps-such as the need for cost-effective co-solvent systems, mechanistic understanding in catalytic applications, and strategies for mechanical reinforcement-thereby offering a roadmap for future research aimed at unlocking the full potential of cellulose aerogels in sustainable technologies.

2 Cellulose

Cellulose is the most abundant and widely distributed natural polymer, and its potential for high-value applications has garnered significant attention from researchers in the fields of chemistry and materials science. As illustrated in Fig. 2, cellulose is a linear polysaccharide homopolymer, characterized by an abundance of highly reactive hydroxyl groups. The intermolecular and intramolecular chains of cellulose are cross-linked through hydrogen bonding, forming supramolecular structures [21–24]. The formation of these supramolecular polymers is predominantly governed by non-covalent interactions, including hydrogen bonds, electrostatic forces, and van der Waals interactions. Due to its unique structural properties, natural cellulose exhibits low density, high durability, exceptional mechanical properties, low production costs, and good biocompatibility. To expand the range of cellulose's applications, researchers frequently employ both physical and chemical modification techniques [25].

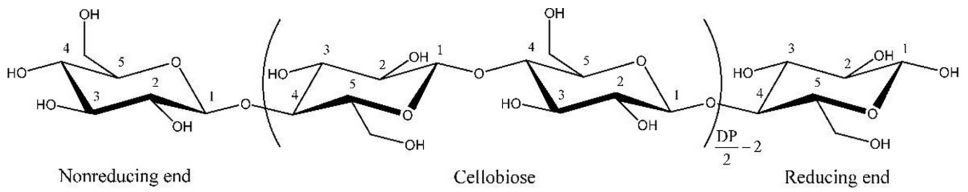

Figure 2: Chemical structure of cellulose.

2.1 Chemical Modification of Cellulose

As shown in Fig. 2, cellulose molecular chains contain abundant hydroxyl functional groups, among which the primary hydroxyl group at position 6 has high reactivity. The commonly used chemical modification methods mainly include esterification, etherification, click chemical modification, carbamate esterification, amidation, silanization modification and polymer grafting [26–29].

2.1.1 Esterification of Nanocellulose

Esterification involves the reaction of the active hydroxyl groups on the macromolecular chains of cellulose with acids, anhydrides, or acyl halides under acidic catalysis, resulting in the elimination of a small molecule and the formation of cellulose esters [30]. Following this reaction, the modification of the hydroxyl groups on the cellulose molecular chains leads to a reduction or complete disruption of hydrogen bonds, weakening both intermolecular and intramolecular interactions. As a result, the cellulose exhibits enhanced thermoplasticity. In industrial applications, acylation reagents, such as acyl chlorides, are commonly used to introduce acyl groups into the cellulose macromolecular chains to produce cellulose esters. Beaumont et al. reported a method for esterification on cellulose surfaces in aqueous solutions, avoiding the need for dewatering or drying processes [31]. The method involves the use of a kneading machine and a reaction at room temperature for 1 h, under mild conditions, making it particularly suitable for industrial applications [31]. Tian et al. synthesized solid fluorescent materials in three primary colors (red, green, and blue) via esterification, where spiropyran, fluorescein, and pyrene were grafted onto cellulose. This modification enabled full-band color development through simple mixing, and by utilizing a fluorescence energy resonance transfer (FRET) strategy, the energy transfer efficiency was modulated, allowing reversible control over the material's color and fluorescence intensity. The modified cellulose-based material demonstrated excellent performance in applications such as information encryption, secure printing, and dynamic anti-counterfeiting [32]. Leszczynska esterified cellulose with succinic anhydride, yielding highly stable modified cellulose. By optimizing reaction time, temperature, and the ratio of succinic anhydride to cellulose, it was observed that an increased ratio of hydroxyl functional groups in the cellulose led to a higher degree of substitution. When the reaction time was extended to 240 min, the maximum proportion of hydroxyl functional groups was reached, significantly reducing the thermal stability of the cellulose. Consequently, highly thermally stable succinylated cellulose can be synthesized by precisely controlling the reaction temperature and esterification degree (Fig. 3a) [33]. Additionally, Nawaz et al. developed a functional cellulose acetate sensor using o-diazepine as the chromophore and diphenylmethane-4,4′-diisocyanate as the linking agent. This sensor exhibited multiple response fluorescence properties, detecting not only amines, such as triethylamine, diethylamine, methylamine, aniline, and benzylamine, but also anions like $B_4O_7^{2-}$, PO_4^{3-} and CO_3^{2-} (Fig. 3b) [34].

Additionally, Jia et al. chemically bonded and grafted fluorescein isothiocyanate (FITC) and protoporphyrin (PpIX) to cellulose acetate (CA) via the highly reactive hydroxyl groups present on the cellulose, resulting in the formation of modified cellulose (CA-FITC and CA-PpIX). By varying the mixing ratios of CA-FITC and CA-PpIX, a tunable solid fluorescent material was produced, whose color could be adjusted from red to green. Notably, the fluorescence emission intensity of this material was found to be linearly related to the logarithm of the amine concentration, enabling it to detect the freshness of seafood (Fig. 3c) [35]. Chen et al. employed dicyclohexyl carbodiimide and 4-dimethylaminopyridine as catalysts to graft porphyrins onto carboxylated nanocellulose (CNC-SA-COOH) through an esterification reaction, successfully producing functionalized cellulose (CNC-SA-$COOC_6$TPP). This porphyrin-functionalized material exhibited high sensitivity and selectivity toward Hg^{2+}, suggesting its potential as a promising fluorescence detection material [36]. Aerogel Implications: Esterification of nanocellulose is a pivotal strategy for engineering the

surface chemistry of aerogels. By replacing hydrophilic hydroxyl groups with hydrophobic acyl chains (e.g., acetyl, succinyl), the modified nanocellulose building blocks impart inherent hydrophobicity to the resulting aerogel network. This directly mitigates the moisture sensitivity of pure cellulose aerogels, preserving their thermal insulation performance in humid environments and enabling selective oil absorption from oil-water mixtures [37]. Furthermore, the introduction of bulky ester groups can disrupt the dense hydrogen-bonding network during gelation, potentially influencing pore size distribution and enhancing mechanical resilience by introducing nanoscale flexibility. The grafting of functional molecules like spiropyran or porphyrins via esterification, as mentioned, transforms aerogels into responsive platforms for sensing and detection, leveraging their high surface area and porous structure for analyte interaction [38,39].

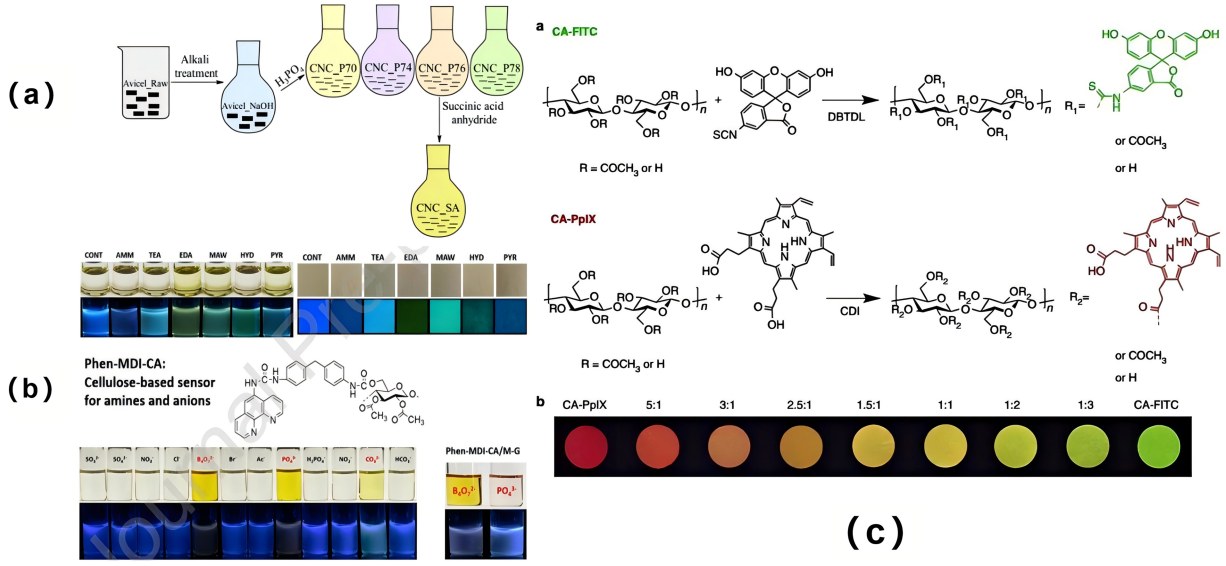

Figure 3: (**a**) The preparation process of modified nanocellulose [33]; (**b**) Fluorescent detection of amine and anions by cellulose [34] Copyright © 2019 Elsevier B. V. All rights reserved. License number (6196450904105); (**c**) Cellulose functionalized by fluorescent groups [35]. Copyright © 2019, The Author(s).

2.1.2 Nanocellulose-Click Chemistry

Filpponen and Argyropoulos were the first to report the modification of nanocellulose using click chemistry [40]. This reaction offers several advantages, including a simple process, mild reaction conditions, no requirement for solvents or the use of easily removed solvents, high product selectivity, minimal by-product formation, a high conversion rate, ease of target product separation, and a low environmental impact. Li et al. utilized the hydroxyl group in ethyl cellulose and the alkyne group in 1-phenyl-2-allyl-1-ketone to successfully synthesize cellulose derivatives modified by phenyl-allyl-ether through a click reaction. Within 5 min, 80% of the substrates were substituted, highlighting the high efficiency of the method (Fig. 4a) [41]. Sun et al. employed a double-click reaction strategy to introduce antibacterial groups into cellulose, achieving functionalization of the material [42]. Initially, under Cu(I) catalysis, a click reaction occurred between the azide group on cellulose and the alkynyl group on propylglycidyl ether (GPE). Subsequently, the propylene oxide on GPE-modified cellulose underwent a ring-opening click reaction with the amino group on polyhexamethylene-monoguanidine phosphate, resulting in the formation of antibacterial group-modified cellulose (CFs-PHMG) (Fig. 4b). CFs-PHMG demonstrated excellent antibacterial activity against *E. coli* and *S. aureus* bacteria and exhibited extremely high stability. Even after storage at room temperature for 2 months, its antibacterial activity remained at 99%. Aerogel Implications: Click chemistry offers a modular

and efficient route for post- or pre-gelation functionalization of nanocellulose aerogels. Its high specificity and yield allow for the precise anchoring of functional moieties (e.g., antibacterial groups, conductive polymers) onto the cellulose scaffold without compromising the porous network's integrity [43]. This method is particularly valuable for creating multifunctional aerogels where the 3D interconnectivity is crucial. For instance, introducing polymer chains via click reactions can act as nanoscale cross-linkers, reinforcing the aerogel's mechanical framework and improving compressive recovery. The modification facilitates the integration of otherwise incompatible components, enabling the fabrication of complex hybrid aerogels with tailored properties for catalysis, sensing, or antimicrobial applications, as detailed in Sections 3.4 and 3.5.

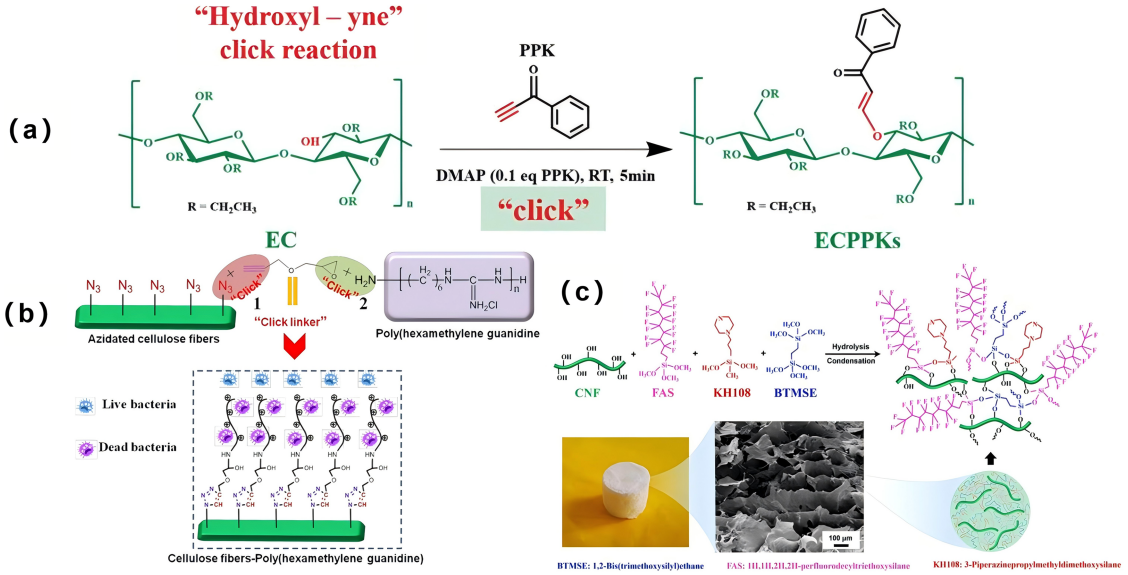

Figure 4: (**a**) Click reaction on the surface of cellulose [41]; (**b**) Ring-opening click modification on the fuctionalized cellulose [42] Copyright © 2020, Springer Nature B. V. License number (6196470582033); (**c**) The application of silanized modification of cellulose in oil-water separation [44]. Copyright © 2021, Springer Nature. License number (6196470820493).

2.1.3 Etherification of Nanocellulose

Etherification refers to the reaction of the alcohol hydroxyl group on the cellulose molecular chain with vinyl groups, halogenated alkyl groups, or etherifying reagents, leading to the formation of cellulose ethers with a high degree of substitution under alkaline conditions. Wu et al. were the first to modify cellulose aerogel with three different silane coupling agents using a one-pot polymerization technique. The modified aerogels exhibited a unique interspersed macroporous structure, excellent compressive properties, and superior oleophilic and hydrophobic characteristics. In an oil-water mixture, the contact angle and water absorption capacity of the material remained stable even after five cycles of absorption and recirculation (Fig. 4c) [44]. Neves et al. successfully modified microcrystalline cellulose by incorporating 3-aminopropyl triethoxysilane in varying proportions. After etherification, the surface properties of the microcrystalline cellulose remained unchanged [45]. Redl et al. used porphyrin radicals to etherify cellulose, anchoring porphyrin molecules onto the cellulose to facilitate molecular switching and the conversion of electrochemical input into chiral optical signals [46]. Silanization, often involving alkoxysilanes like MTMS or VTMS, is one of the most effective methods to render nanocellulose aerogels hydrophobic and oleophilic [37,47]. The silane coupling agents form covalent Si-O-C bonds with cellulose hydroxyls and self-condense into a polysiloxane network, coating the nanofibrils. This nano-coating significantly reduces surface energy, leading to high

water contact angles (>150°) while maintaining the mesoporous structure essential for high adsorption capacity. Crucially, this conformal coating strengthens the nanofibril joints, often improving the aerogel's mechanical robustness and elastic recovery under compression, as demonstrated in superelastic aerogels for oil-water separation [48,49]. This direct link between molecular-scale grafting and macro-scale aerogel performance underscores the importance of surface modification.

2.1.4 Graft Copolymerization Modification of Nanocellulose

Copolymerization modification involves the reaction of the hydroxyl groups on the nanocellulose molecular chains with a polymer, introducing a polymer chain with distinct properties, resulting in the formation of a polymer-modified and grafted cellulose material. This modification not only enhances the dispersion stability of nanocellulose in both polar and non-polar media, but also imparts unique functionalities. The graft copolymerization of cellulose can be classified into two types: heterogeneous and homogeneous. Heterogeneous graft copolymerization typically occurs under heterogeneous conditions, where the reactant and medium form a two-phase or multiphase system, such as in suspension polymerization, emulsion polymerization, reverse suspension polymerization, and reverse emulsion polymerization. However, due to the extensive hydrogen bonding between cellulose molecules, the modified reactant is often unable to penetrate the crystalline regions of cellulose. Consequently, in heterogeneous grafting, the number of grafted side chains on the cellulose macromolecules is typically lower. In contrast, homogeneous graft copolymerization requires that both the reactants and media be dissolved into a homogeneous system, resulting in a more uniform distribution of modified cellulose macromolecular chains and a higher number of grafted cellulose macromolecules [50,51].

2.1.5 Modification of Nanocellulose by Free Radical Polymerization

Free radical and ion-induced grafting are commonly used methods for modifying nanocellulose. However, free radical polymerization has several drawbacks, such as the difficulty in precisely controlling the reaction course, the molecular weight of the product, and the length of the graft chains. To address these limitations, reversible deactivation techniques such as Reversible Addition-Fragmentation Chain Transfer (RAFT), Nitroxide Mediated Polymerization (NMP), and Atom Transfer Radical Polymerization (ATRP) have garnered increasing attention. Barsbay and Güven successfully grafted vinyl monomers onto lignin via RAFT grafting polymerization in an aqueous solution. Furthermore, free radical polymerization was used to induce phenol reactions with lignin in jute fabric, resulting in the formation of modified jute fabric polymers [52]. Meng et al. successfully acylated cellulose at room temperature using Atom Transfer Radical Polymerization. The reaction involved 1-allyl-3-methylimidazole chloride as an ionic liquid to polymerize methyl methacrylate and cellulose with styrene, without the need for catalysts or protective groups (Fig. 5b) [50].

2.1.6 Silanization of Cellulose

Silane, due to its low cost, has been widely utilized as a coupling agent in composite materials. Silanes containing active functional groups can form cross-links with composites through covalent or van der Waals forces [53]. Additionally, the silanized surface of nanocrystalline cellulose is hydrophobic, which enhances its dispersibility in organic or low-polarity solvents. The coupling of silane with nanocrystalline cellulose typically occurs in two steps: first, silane undergoes hydrolysis to form silanol, and then the silanol condenses with the hydroxyl groups on the nanocrystalline cellulose. Zhu et al. prepared cellulose hydrogels by subjecting nanocrystals, with varying mass fractions (1–3 wt%), to ultrasonic treatment for 5 min. Subsequently, 3-(2-aminoethyl aminopropyl dimethoxy-methylsilane) (AEAPMDS) at different mass

fractions (2, 4, 6, 8, and 10 wt%) was added for reaction. After t reatment w ith h ot w ater, tert-butanol exchange, and other steps, silanized nanocellulose was obtained. The modified cellulose hydrogels exhibited high CO_2 adsorption capacity (Fig. 5c) [54]. Yang and Pan introduced highly active amino functional groups onto cellulose via a silanization reaction, followed by reaction with fluorescein isothiocyanate or N-hydroxysuccinimide 1-pyrene butyrate to successfully incorporate fluorescence emission groups. This material demonstrated excellent fluorescence emission properties (Fig. 5d) [55]. Moreover, the method is versatile: when applied to other cellulose substrates, materials with similarly outstanding fluorescence emission characteristics can be synthesized. Lucia et al. employed cellulose dialdehyde (DAC) as a derivative and reacted it with (3-amino-propyl) triethoxysilane. Through different processing conditions, they obtained silane compounds with varying degrees of hydrolysis [56].

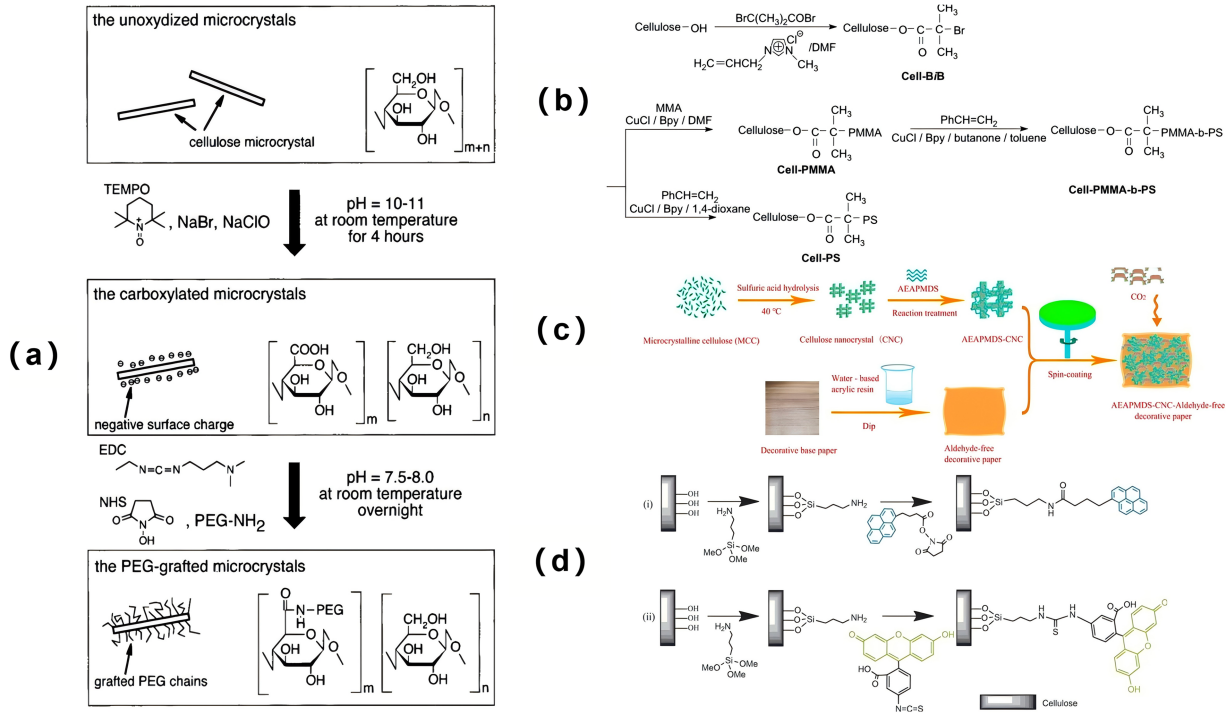

Figure 5: (**a**) The preparation process of PEG-functionalized cellulose [57]. Copyright © 2001 American Chemical Society. License number (6196480284048); (**b**) Atom transfer radical polymerization modification of cellulose [50]; (**c**) The flow chart of silanized modified nanocellulose hydrogel [54]; (**d**) The preparation process of cellulose of functionalized by fluorescence groups [55]. Copyright © 2010 Wiley Periodicals, Inc. License number (6196480808807).

2.1.7 Amidation of Cellulose

Amidation is a widely used method for surface modification of cellulose, typically catalyzed by sulfuric acid or hydrochloric acid to facilitate the conjugation of carboxyl and amino groups. Araki et al. prepared cellulose through acid hydrolysis, followed by TEMPO oxidation treatment and subsequent grafting of PEG-NH2 onto the cellulose via acylation. Characterization using thermogravimetric analysis and infrared spectroscopy revealed that approximately 20%–30% of the carbonyl functional groups in the modified cellulose participated in the amidation reaction. After PEG grafting, the dispersion stability of cellulose was significantly improved, and even after freeze-drying treatment, the modified cellulose could be re-dispersed in water or chloroform. This improvement in dispersibility provides strong support for the material's potential industrial applications (Fig. 5a) [57]. Aerogel Implications: Amidation introduces carboxyl or

amine functionalities onto nanocellulose, dramatically altering its surface charge and interaction potential. In aerogel formation, this enhances the dispersibility of nanocellulose in various solvents, leading to more homogeneous gels and, consequently, aerogels with uniform pore structures. The introduced ionic groups (e.g., $–COO^–$, $–NH_3^+$) can facilitate electrostatic cross-linking or enable the electrostatic assembly of oppositely charged nanomaterials (e.g., graphene oxide, MOFs) into hybrid aerogels with hierarchical pores [58,59]. Furthermore, these functional groups serve as active sites for anchoring catalytic nanoparticles or dye molecules, directly contributing to the aerogel's application in catalysis and adsorption, as discussed in Sections 3.4 and 3.5 [60,61].

2.2 Physical Modification of Cellulose

Physical modification refers to the enhancement of the diffusion and penetration capabilities of reactants in cellulose through processes such as microspherification, micropulverization, or film processing [58]. Common methods of physical modification include ammonia blasting, electron beam radiation, high-pressure beating, solvent exchange, and dry or wet ball milling. Among these, the ball milling method has become one of the most widely employed techniques due to its broad applicability and relatively low cost. Compared to chemical modification, physical modification offers several advantages, including milder reaction conditions, simpler operation, environmental sustainability, and feasibility, making it more suitable for industrial applications and widespread adoption [62,63].

Non-covalent modification of cellulose through polymer adsorption can impart new functionalities to the material. This approach has found widespread application in the papermaking industry, where it enhances the mechanical properties of paper. The functional molecules typically modified by cellulose adsorption include polymer electrolytes and non-ionic polymers [64]. Xia et al. synthesized an amphiphilic copolymer composed of hydrophilic methoxy-polyethylene glycol (MPEG) and hydrophobic polydimethylsiloxane (PDMS), which was physically adsorbed onto cellulose nanocrystals via non-covalent interactions. When the modified cellulose was mixed with silicone oil, the compatibility between the two was significantly improved, and the method also enhanced the viscosity of the silicone oil [65]. Sun et al. integrated multiple stimuli-such as photochromic, wet chromic, thermochromic, and electrochromic properties-into a series of light-emitting 1,8-naphthalenediimide-violet binary compounds. These compounds exhibited unique double photochromic and wet chromic switching behaviors when embedded in a cellulose matrix in the solid state. The material demonstrated reversible solid-state fluorescence hydrochromism with changes in relative humidity and reversible solid photochromism upon the formation of stable violet radical cations. Moreover, these dyes could be printed onto cellulose paper via inkjet printing or cast into thin films based on cellulose powder, allowing for a one-way cyclic transition between three distinct states, thus enabling visualization under ultraviolet or visible light [66]. Wendler et al. reported that, compared to N-methylmorpholin-n-oxide-hydrate (NMMO), which is commonly used as a solvent, ionic liquids offer better solubility for cellulose, higher thermal stability, and superior chemical tolerance. Cellulose form can be controlled through physical modification via ionic liquid dissolution [67]. Aerogel Implications: Physical modification methods like ball milling primarily affect the morphology and aspect ratio of nanocellulose, which are critical parameters governing aerogel microstructure. Longer, more flexible nanofibers (CNFs) tend to form entangled networks leading to smaller, more numerous pores and higher mechanical strength, while shorter nanocrystals (CNCs) create more brittle structures with different pore geometries. Techniques like ammonia blasting or ionic liquid treatment can partially decrystallize cellulose, increasing amorphous regions and enhancing solubility. This allows for the regeneration of cellulose II aerogels, which often exhibit different mechanical and adsorption properties compared to native cellulose I aerogels [68,69]. Controlling

the nanocellulose precursor's physical state is thus a fundamental first step in tailoring the aerogel's density, porosity, and mechanical performance.

2.3 Influence of Cellulose Source on Aerogel Pore-Forming Mechanism

The pore architecture of nanocellulose aerogels is profoundly influenced by the intrinsic properties of the cellulose source, including aspect ratio, crystallinity, and surface charge. These parameters dictate the assembly behavior during gelation and the final porous morphology.

Aspect ratio: Nanocellulose with high aspect ratio, such as cellulose nanofibrils (CNFs, length >1 μm, diameter 2–20 nm), tends to form entangled networks through physical intertwining and hydrogen bonding, leading to aerogels with smaller, more numerous pores and enhanced mechanical strength. In contrast, cellulose nanocrystals (CNCs, length 100–250 nm, diameter 5–70 nm), with lower aspect ratios, assemble into more brittle structures with larger, irregular pores due to limited fiber entanglement [70,71]. Bacterial nanocellulose (BNC) exhibits an ultrafine, high-aspect-ratio fibrillar network, often resulting in aerogels with hierarchical, well-interconnected pores and high transparency.

Crystallinity: Highly crystalline CNC (crystallinity >80%) contributes to rigid network junctions, favoring the formation of micropores (<2 nm) and enhancing thermal stability. However, excessive crystallinity may reduce flexibility and limit pore connectivity. Partially amorphous CNFs or regenerated cellulose (cellulose II) contain more disordered regions, which promote swelling and solvent retention during gelation, leading to mesoporous (2–50 nm) and macroporous (>50 nm) structures with improved compressibility [59,72].

Surface charge: The surface charge, often modulated by chemical pretreatment (e.g., TEMPO-oxidation, sulfonation), affects colloidal stability and inter-fibril repulsion during gelation. Highly charged nanocellulose (e.g., TEMPO-oxidized CNF, zeta potential < −30 mV) exhibits strong electrostatic repulsion, facilitating homogeneous dispersion and forming aerogels with narrow pore size distribution [73]. Conversely, low surface charge may lead to aggregation and heterogeneous pore formation. The introduction of anionic groups ($-COO^-$) or cationic modifications ($-NH_3^+$) further enables electrostatic cross-linking or interaction with oppositely charged additives (e.g., graphene oxide, MOFs), creating hybrid aerogels with tailored pore hierarchies [74,75].

These source-dependent characteristics underscore the importance of selecting appropriate nanocellulose types for targeted applications. For instance, CNF-based aerogels are suitable for mechanical reinforcement and adsorption, whereas CNC-based systems benefit catalytic supports requiring high surface area. This understanding bridges the gap between raw material selection and aerogel microstructure, providing a guideline for reproducible and application-specific design. Nevertheless, achieving an ultrahigh specific surface area often comes at the expense of mechanical robustness. For instance, aerogels with porosity >99% and specific surface areas exceeding 500 m^2/g tend to exhibit fragile frameworks, limiting their applicability in load-bearing or cyclic environments. The aspect ratio and crystallinity of nanocellulose play pivotal roles in this balance: long, flexible CNFs can form entangled networks that better withstand deformation, whereas short, rigid CNCs yield more brittle structures despite their high surface area. Similarly, excessive chemical modification (e.g., oxidation) can introduce excessive surface charge and repulsion, leading to highly porous but mechanically weak gels. Therefore, the selection of cellulose source must align with the performance priorities of the intended application—for example, CNF-based aerogels are preferable for compressive recovery, while CNC-based systems may be optimized for catalytic supports where surface area is paramount.

2.4 Influence of Drying Methods Impact on Aerogel Properties

The final step in aerogel production is the removal of solvent from the wet gel while preserving its porous architecture. The choice of drying technique profoundly influences the pore structure, mechanical stability, specific surface area, and overall performance of the resulting aerogel, as well as its production cost and scalability. The three most common drying methods-freeze-drying, supercritical drying, and ambient pressure drying (as summarized in Table 1), each present distinct advantages and limitations, which must be considered in relation to the target application.

Table 1: Comparison of common drying methods for nanocellulose aerogels.

Drying Method	Freeze Drying	Supercritical Drying	Ambient Drying
Typical porosity	90%–99%	95%–99.8%	85%–95%
Pore structure stability	Moderate; ice-crystal artifacts possible	Excellent; minimal shrinkage, uniform nanopores	Good with chemical pretreatment; some shrinkage
Specific surface area (typical)	100–400 m^2/g	300–600 m^2/g	50–300 m^2/g
Cost & scalability	Moderate cost; lab-scale friendly; limited scalability	High cost; specialized equipment; low throughput	Low cost; highly scalable; short cycle time
Recommended applications	Adsorbents, biomedical scaffolds, insulation	High-end insulation, catalyst supports, sensors	Industrial absorbents, packaging, composites

Freeze-drying (lyophilization) involves freezing the wet gel and subsequently sublimating the ice under vacuum. This method typically yields aerogels with high porosity (≈90%–99%) and a hierarchical pore structure containing both mesopores and macropores. However, the growth of ice crystals can sometimes cause partial pore-wall collapse or irregular pore shapes, especially if the freezing rate is not controlled [76]. Freeze-dried aerogels generally exhibit moderate specific surface areas (100–400 m^2/g) and good mechanical resilience, though they may be comparatively brittle. The process is relatively low-cost at laboratory scale and does not require high-pressure equipment, but the long processing time (24–72 h) and energy consumption during prolonged vacuum operation limit its industrial throughput [77]. Freeze-drying is widely adopted for biomedical scaffolds, adsorbents, and thermal insulators where interconnected macroporosity is beneficial, and where the balance between performance and cost is acceptable.

Supercritical drying (usually with CO_2) avoids liquid-vapor interfaces by bringing the solvent to a supercritical state, thereby eliminating capillary forces that cause pore collapse. This method produces aerogels with exceptionally high specific surface areas (300–600 m^2/g), uniform nanoporosity, minimal shrinkage, and excellent structural fidelity [18,78]. The resulting materials often show superior thermal insulation, mechanical strength, and pore stability. Nevertheless, supercritical drying demands specialized high-pressure equipment, involves significant operational costs, and requires extensive solvent exchange prior to drying [79]. It is therefore a high-cost, low-throughput technique reserved for applications where

extreme porosity, precise pore control, or exceptional performance are critical, such as in advanced thermal barriers, catalyst supports, or high-sensitivity sensors.

Ambient pressure drying is the most economical and scalable approach, where the solvent is evaporated at room or slightly elevated temperature [80]. To reduce capillary stresses, the gel is usually subjected to prior solvent exchange with low-surface-tension liquids (e.g., tert-butanol, acetone) and/or chemical modification (e.g., silylation) to reinforce the pore walls. Aerogels dried under ambient conditions often show higher density, lower porosity (≈85%–95%), and some shrinkage, leading to moderate specific surface areas (50–300 m^2/g) [81,82]. Recent advances in precursor cross-linking and solvent-exchange protocols have enabled ambient-dried nanocellulose aerogels with improved pore stability and acceptable performance. This method is particularly attractive for large-scale production of absorbents, packaging materials, or composite fillers, where cost-effectiveness and production speed outweigh the need for ultra-high porosity.

The choice of drying method not only dictates porosity and surface area but also directly influences the mechanical durability of nanocellulose aerogels. Freeze-dried aerogels, while highly porous, often exhibit microcracks and irregular pores due to ice-crystal growth, leading to reduced compressive recovery after repeated loading. Supercritical-dried aerogels achieve the highest specific surface areas and uniform nanoporosity, yet their networks can be brittle, with limited elastic recovery under large strains. In contrast, ambient-dried aerogels, though possessing lower porosity, typically show higher density and improved mechanical robustness due to reduced capillary collapse and the potential for in-situ cross-linking during solvent exchange. Therefore, applications requiring long-term durability (e.g., reusable adsorbents, wearable sensors) may benefit from ambient drying with tailored cross-linkers, whereas ultra-high-surface-area applications (e.g., catalyst supports) may prioritize supercritical drying despite its mechanical limitations.

3 Cellulose Based Aerogel

Aerogels can be broadly classified into three categories based on the materials used in their synthesis: inorganic, organic, and organic-inorganic hybrid aerogels. Traditional inorganic aerogels, such as silica aerogels, exhibit a high degree of porosity and specific surface area. However, their pore structure is prone to collapse, which limits their utility in manufacturing and storage applications. To address these limitations and meet the growing demand for sustainable, robust, and multifunctional porous materials, research has increasingly focused on biopolymers. Among these, cellulose stands out as a premier candidate due to its natural abundance, renewability, biodegradability, and excellent intrinsic mechanical properties. Cellulose, a pure organic biomass polymer, is characterized by its abundant hydroxyl groups, low thermal expansion coefficient, excellent mechanical properties, and high optical transparency. Due to the presence of numerous highly reactive hydroxyl groups, cellulose can be functionalized through chemical modifications such as etherification, grafting, and crosslinking, as well as the introduction of carboxyl, sulfonic, and amino groups. Consequently, cellulose has become a widely utilized material in the preparation and synthesis of aerogels [83]. Compared to traditional aerogels, such as SiO_2, carbon, and TiO_2, nanocellulose aerogels exhibit superior resistance to brittleness. They also possess favorable characteristics, including hydrophilicity (while remaining insoluble in water), excellent mechanical properties, biocompatibility, and biodegradability [84–86]. The properties of nanocellulose aerogels can be dramatically expanded through hybridization and composite formation. The chemical and physical modification strategies detailed in Section 2 provide the essential toolkit for this purpose. For instance, hydrophobically modified nanocellulose forms the backbone of oleophilic aerogels for oil spill remediation. Conversely, introducing charged groups via amidation enables the electrostatic assembly of functional guests like graphene oxide or MOFs. Using cellulose as a functionalizable scaffold, and incorporating organic polymers, inorganic materials, metals, or metal oxides as guest substances, it is possible to synergistically preserve the inherent advantages of cellulose-such as

its mechanical strength, degradability, and non-toxicity-while also enhancing its physical and chemical properties to impart specific functionalities. This approach significantly broadens the application potential of cellulose-based aerogels [3,87]. These functionalized cellulose and regenerated cellulose aerogels have found widespread use in various fields, including antibacterial applications, water purification, catalysis, separation processes, bioengineering, medical diagnostics, and photonic devices, demonstrating substantial promise for future applications [88–90]. We have summarized and discussed the functionalized part of the nanocellulose composite aerogel in the form of a table, which is shown in Table 2 below:

Table 2: Functionalization of nanocellulose composite aerogels.

Raw Materials of Aerogel	Preparation Method	Composite Aerogel Properties	Ref.
SiO_2 CNF	Sol-gel method, Freeze-drying method	Compression modulus 12.43 MPa, compressive strength 2.59 MPa	[91]
GO TOCNF	Two-way freezing method, freeze-drying method	Plastic deformation of 0.1% and 8.2% at 20% and 50% strain (1×10^4 compression cycles)	[92]
PVA GA CNF	Hydrothermal method, freeze-drying method	Thermal conductivity 0.044 ± 0.005 W/m K thermal diffusivity 0.333 ± 0.001 mm^2/s (30°C)	[93]
GNS PANI TOCNF	*In situ* polymerization technology freeze-drying method	Electrical conductivity 11.78 S/cm	[94]
OA Fe_3O_4 CNF	Physical Mixing freeze-drying method	Saturation magnetization value 53.69 emu/g	[95]
AgNPs Chitosan CMC	Coaxial 3D Printing Technology reeze-drying method	Effectively inhibits the proliferation of *Escherichia coli* and *Staphylococcus aureus*	[96]
Protein hydrolase AgNPs CNF, TO-CNF cationic CNF	Freeze-drying method	Inhibits the growth of 92% of bacteria (*E. coli*).	[97]

3.1 Silica-Cellulose Based Aerogel

Silica aerogels, one of the earliest types of aerogels, are typically prepared from silica gel in a specific solvent, followed by CO_2 supercritical drying. Although cellulose aerogels exhibit excellent thermal insulation properties, their hydrophilic nature allows them to absorb moisture from the surrounding air, which can negatively affect their thermal performance. In contrast, silica aerogels are considered highly efficient insulating materials due to their exceptionally low thermal conductivity. The incorporation of silica into cellulose aerogels effectively mitigates moisture absorption, thereby preserving their thermal insulation capabilities. Demilecamps et al. synthesized cellulose–SiO_2 aerogels by introducing polyoxodisiloxane (PEDS) into a cellulose–alcohol gel, employing both molecular diffusion and forced flow induction methods. The aerogels produced by these two methods exhibited low thermal conductivities of 0.026 and 0.028 W/(m·K),

respectively. While the thermal conductivity of the cellulose–SiO_2 aerogels was increased by 11% compared to pure SiO_2 aerogels, their tensile strength was enhanced by 25%–40%, making them more suitable for industrial applications [98].

3.2 Graphene-Cellulose Based Aerogel

Graphene and its derivatives, including reduced graphene oxide (rGO) and graphene oxide (GO), have been extensively studied as additives in cellulose aerogels. The incorporation of graphene into aerogels can enhance their resistance to water and improve their electrical conductivity. The resulting composite aerogels, which combine graphene with cellulose, exhibit significant advantages and potential across various applications. Wang et al. utilized the high aspect ratio and negative charge characteristics of nanocellulose to separate graphene oxide sheets through steric hindrance and electrostatic repulsion, eliminating the need for chemical linkers. This innovative approach not only simplifies the preparation process but also enhances the material properties. The composite aerogels demonstrate excellent adsorption capabilities, with maximum adsorption capacities of 111.2 mg/g for methylene blue and 47.3 mg/g for tetracycline, highlighting their promising application in water purification [99]. Wu et al. prepared graphene-cellulose-based aerogels by incorporating graphene into bacterial cellulose and applied them to light, heat, and electricity conversion. Their studies revealed that adding 0.5 wt% graphene to bacterial cellulose increased the thermal conductivity from 0.3 to 1.17 W/(m·K), enhanced the energy storage capacity by 96%, and achieved a photothermal energy conversion output power of 1.8 mW with a maximum photothermal conversion efficiency of 90.3% (Fig. 6) [100]. Yao et al. obtained graphene-composite cellulose aerogels via ultrasonic self-assembly of nanocellulose and graphene in a one-pot process. This three-dimensional aerogel structure is formed by the interconnection of two-dimensional graphene nanosheets and multiple hydrogen bonds in nanocellulose, resulting in strong adsorption and degradation effects on antibiotics, with a removal efficiency exceeding 69%. The adsorption process is primarily driven by electrostatic attraction, π-π interactions, and hydrogen bonding [101].

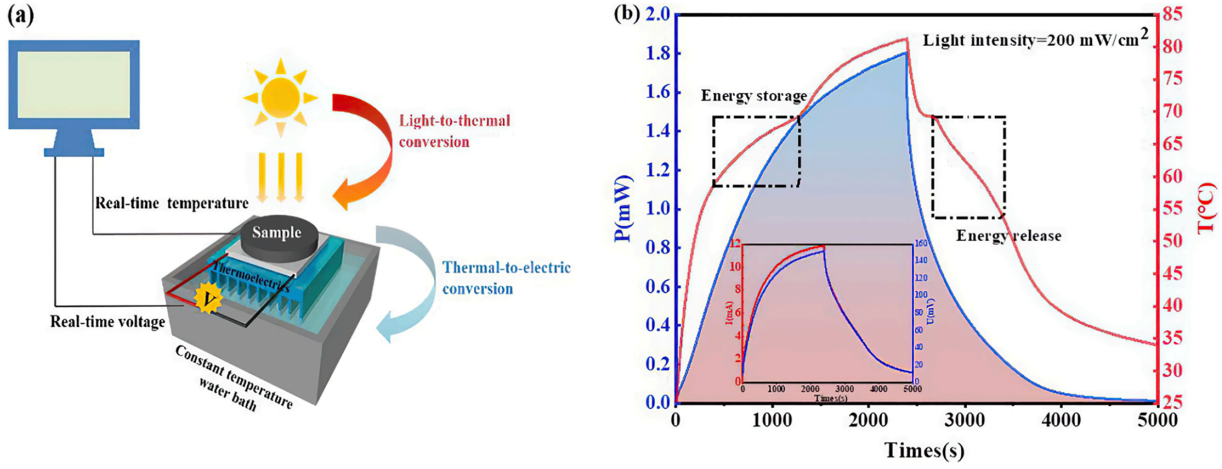

Figure 6: Self-made thermoelectric sensing device and sample thermoelectric conversion curve, (**a**) Schematic diagram of self-made thermal difference device. (**b**) Thermoelectric conversion curve of sample (inset: the variation curve of voltage and current with time) [100]. Copyright © 2022 Elsevier Ltd. All rights reserved. License number (6196481158391).

3.3 Polymer-Cellulose Based Aerogel

Polymers are typically categorized into inorganic and organic types and are commonly employed as additives to modify the properties of cellulose aerogels [102]. Polypyrrole (PPy) and polyvinyl alcohol (PVA) are two widely used organic polymers. Zhuo et al. prepared a polypyrrole/cellulosic carbon composite aerogel supercapacitor in a 1 M H_2SO_4 solution. The integration of conductive polymers, such as polypyrrole (PPy) and polyaniline (PANI), represents a prominent strategy to endow inherently insulating cellulose aerogels with electrochemical activity for energy storage applications. This functionalization leverages the high porosity of the cellulose scaffold for efficient ion transport and the conductive polymer for charge storage via faradaic reactions. Zhuo et al. provided a compelling case study by preparing a polypyrrole/cellulosic carbon composite aerogel (Cell@PPy) supercapacitor. As illustrated in Fig. 7, the electrochemical characterization-including cyclic voltammetry curves with distinct redox peaks (Fig. 7a,d) and nearly triangular galvanostatic charge-discharge profiles (Fig. 7b,e)-confirms the successful integration of PPy and the hybrid material's capacitive behavior. The composite achieved a high specific capacitance of 387.6 at 0.5 A/g and an outstanding cycling stability of 92.6% capacitance retention after 10,000 cycles [93]. This performance is competitive within the landscape of polymer-cellulose aerogels for supercapacitors. For instance, as summarized in Table 2, polymer-cellulose aerogels can achieve specific capacitances in the range of several hundred F/g. The value reported for Cell@PPy compares favorably and highlights how the *in-situ* polymerization of PPy on a conductive cellulosic carbon aerogel scaffold creates a synergistic architecture conducive to both electrical conductivity and ionic accessibility. Other works, such as the incorporation of polyaniline (PANI) with graphene and TEMPO-oxidized cellulose nanofibrils (TOCNF), have also yielded aerogels with high conductivity (up to 11.78 S/cm) suitable for electrode materials, underscoring the versatility of the polymer hybridization approach [103]. These examples collectively demonstrate that polymer functionalization is a potent tool for expanding cellulose aerogels into the realm of flexible and sustainable electroactive devices.

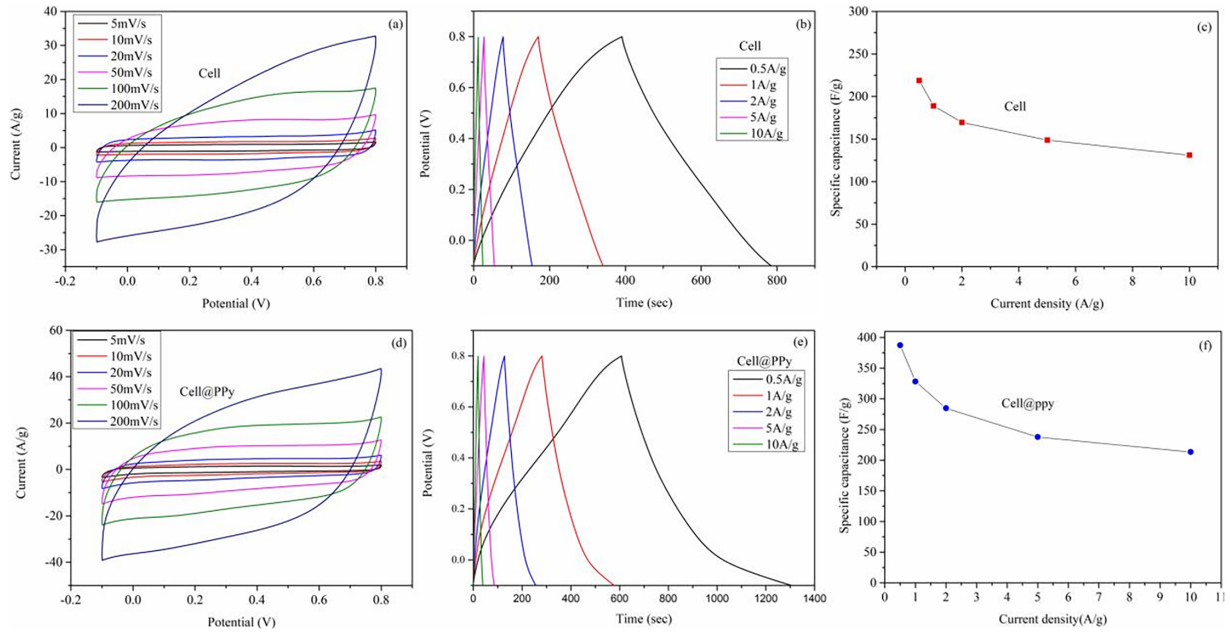

Figure 7: (**a**,**d**) Cyclic voltammetry curves of cell and polypyrrole/cellulosic carbon aerogel (Cell@PPy); (**b**,**e**) Charge and discharge of the battery; (**c**,**f**) Specific heat capacity [93]. Copyright © 2019 Elsevier Ltd. All rights reserved. License number (6196490600425).

Chitosan and alginic acid are two common organic polymers that, like cellulose, are derived from renewable and biodegradable natural sources. Chitosan is produced by deacetylation of chitin, which is abundantly available from crustacean shells and fungal biomass, and is recognized for its biocompatibility, biodegradability, and non-toxicity [104]. Similarly, alginic acid is a natural polysaccharide extracted from brown seaweed (e.g., *Laminaria* spp.) and is widely used in biomedical and environmental applications due to its renewable origin, biodegradability, and gel-forming ability [105]. These intrinsic properties, coupled with their renewable sourcing and ecological safety, make chitosan and alginic acid highly suitable for the preparation of sustainable cellulose-based aerogel materials. Pan et al. successfully prepared cellulose-chitosan composite aerogels using a high-concentration ionic liquid, LiBr, in combination with co-solubilization and renewable processes. In this composite aerogel, cellulose serves to construct the porous structure and enhance the mechanical strength, while chitosan provides amino reaction sites and adsorbs formaldehyde through chemical bond anchoring. The resulting cellulose-chitosan composite aerogel exhibits a high pore structure and a large specific surface area of 245 m^2/g [106]. The results demonstrate that when the mass ratio of chitosan to cellulose is 1:2, the composite aerogel can rapidly and irreversibly adsorb formaldehyde, with an adsorption capacity of up to 7.5 mmol/g (224 mg/g), indicating excellent adsorption performance.

Zhang et al. prepared cellulose type II aerogels in LiBr solution through dissolution and regeneration strategies. The resulting pure cellulose aerogel exhibits a high pore structure, a large specific surface area (221.3 m^2/g), and excellent flexibility. By varying the chitosan content in cellulose, they observed that when the cellulose-to-chitosan ratio was 1:8, the voltage output increased by 269%, and when the ratio was 1:2, the voltage output rose by 311%. These findings suggest that chitosan enhances the voltage output capacity of the aerogel material [107]. Additionally, the authors investigated the combination of cellulose and alginate-based aerogels and found that the incorporation of alginate also significantly improved the voltage output. These results indicate that the introduction of electron-absorbing or electron-donating polysaccharide polymers into cellulose can enhance the electrical properties of the material. This composite aerogel shows promising potential for applications in fields such as power calculation, light-emitting diodes (LEDs), capacitors, and human motion monitoring.

3.4 Semiconductor-Cellulose Based Aerogel

Integrating semiconductors (e.g., TiO_2, BiOBr) with nanocellulose aerogels creates advanced functional materials where the cellulose scaffold plays an active role beyond mere support [108]. The synergy lies in combining the photocatalytic/photothermal activity of semiconductors with the high porosity, surface reactivity, and design flexibility of cellulose aerogels. A key advantage is using cellulose as a bio-template to control semiconductor morphology and dispersion, preventing nanoparticle aggregation [109].

For instance, Zhou et al. synthesized flower-like BiOBr/microcrystalline cellulose (BiOBr/MCC) composites via an *in-situ* method (Fig. 8). The hydroxyl groups on cellulose coordinated with Bi^{3+} ions, templating the growth of interconnected BiOBr nanosheets [108]. This unique petal-like morphology provides a high surface area and enhances light harvesting through multiple internal reflections, leading to superior adsorption and visible-light photocatalytic degradation of Rhodamine B. The primary mechanism involves pollutant adsorption onto the cellulose matrix followed by oxidation by photogenerated holes (H^+). This case exemplifies how cellulose directs semiconductor architecture for improved performance.

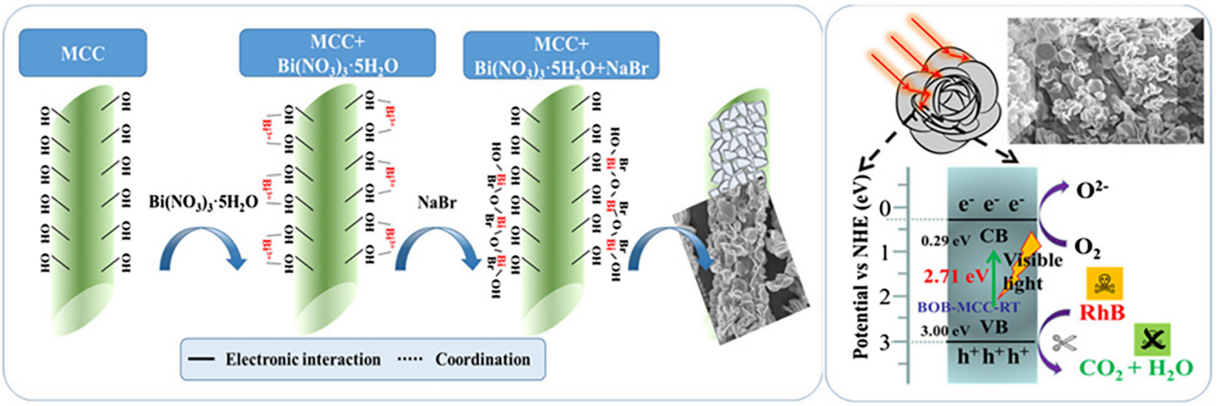

Figure 8: Schematic illustration of the morphology and photocatalytic performance of semiconductor-cellulose composite aerogels.

The surface chemistry of cellulose is crucial for interfacial engineering. Maimaiti et al. grew TiO_2 nanoparticles on ethylenediamine-functionalized nanocellulose (TiO_2/NCC-EDA) [110]. The aminated surface improved TiO_2 dispersion, enhanced CO_2 adsorption, and facilitated charge separation, resulting in efficient photocatalytic CO_2 reduction to methyl formate (yield: 68.3%). Furthermore, semiconductor-cellulose aerogels are expanding into photothermal applications. In a recent study, a conjugated polymer (PM6) was coated on a CNF/PDMS aerogel, creating a bilayer evaporator. The PM6 layer provided strong light absorption (>95%), while the cellulose-based scaffold ensured mechanical robustness and efficient water transport. This synergy achieved a high solar evaporation rate of 2.53 kg m^{-2} h^{-1} with 98.1% efficiency, demonstrating the versatility of these hybrids for solar-driven desalination.

In summary, semiconductor-cellulose aerogels leverage cellulose as a structural director, dispersant, and functional modifier. The enhanced performance originates from tailored semiconductor morphology, improved interfacial charge transfer, and the hierarchical porous network of the aerogel. This aligns with the functionalization strategies in Section 2 and the performance trends summarized in Table 2. Future work should focus on elucidating interfacial charge kinetics and developing scalable fabrication for applications in environmental remediation and energy conversion.

3.5 Cellulose-Based Aerogel Composite with Other Materials

To further enhance the performance of cellulose-based materials, researchers frequently incorporate other functional materials, such as functional molecules, metal-organic frameworks (MOFs), and metal nanoparticles [111]. Seo et al. physically mixed UiO-66 and TEMPO-oxidized cellulose nanofibers (TOCN), and even with a MOF loading as high as 50%, the resulting aerogel maintained high stability. The functionalized cellulose aerogel exhibited a high specific surface area of 483 m^2/g and demonstrated the ability to degrade nerve agents efficiently [112]. Zou et al. synthesized a dopamine-complexed cellulose-based aerogel (PDA-CA), which exhibited strong hydrophilic properties. Under sunlight, the solar evaporation rate of the aerogel reached 1.36 kg·m^{-2}·h^{-1}, indicating excellent seawater evaporation efficiency. Moreover, PDA-CA displayed significant adsorption capacity for organic dyes [113]. Shi et al. polymerized pyrrole monomer onto nanocellulose via vapor phase polymerization, producing a black NCG/PPy composite material. To assess the neural repair potential of the NCG/PPy composites, they utilized PC12 cells in their studies. The experimental results demonstrated that the pyrrole-loaded nanocellulose exhibited enhanced nerve repair capabilities, primarily due to the improved electrical conductivity of the NCG/PPy composite. Under

electrical stimulation, the material facilitated nerve duct formation, mimicking the conduction properties of nerve myelin, thereby promoting nerve growth and axon regeneration, and ultimately contributing to nerve injury repair (Fig. 9a) [114].

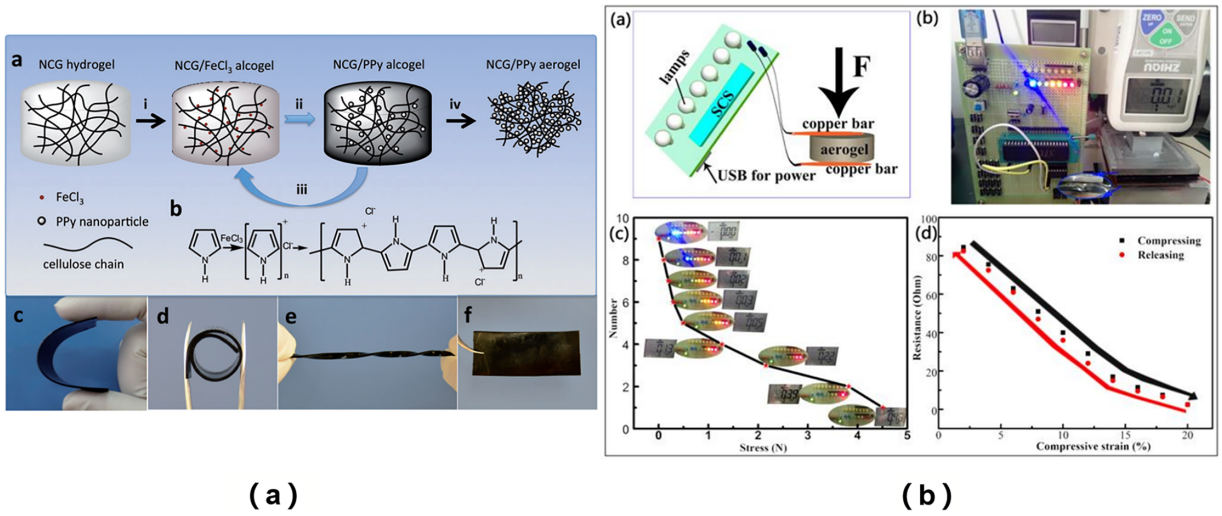

Figure 9: (**a**) The synthesis process of NCG/PPy composite aerogel [114]. Copyright © 2014 WILEY-VCH Verlag GmbH & Co. KGaA, Weinheim. License number (6196490050541); (**b**) The pressure sensing responsiveness test on Ag/CNF [115]. Copyright © 2017 Elsevier Ltd. All rights reserved. License number (6196490301274).

Yao et al. demonstrated the anchoring of silver (Ag) nanoparticles onto nanocellulosic aerogel (Ag/CNF) via multiple hydrogen bonding interactions. This approach imparts the material with exceptional structural stability, as evidenced by its ability to rapidly recover its aerogel structure after undergoing 100 cyclic compression tests, thereby highlighting its robust compressive properties. Additionally, the composite exhibited an extremely sensitive stress-sensing response (Fig. 9b) [115]. Matsuyama et al. successfully synthesized a highly dispersed composite cellulose aerogel containing silver nanoparticles using CO_2 supercritical drying technology. This material displayed excellent antibacterial efficacy against *Escherichia coli* and *Aspergillus niger*, which can be attributed to the uniform dispersion of Ag nanoparticles within the aerogel, significantly enhancing its antibacterial properties [116].

3.6 Systematic Comparison of Hybrid/Composite Aerogels and Their Performance Metrics

Table 3 illustrates how hybridization tailors aerogel properties for targeted applications. Silica-cellulose aerogels combine the low thermal conductivity of silica with the mechanical toughness of cellulose, making them suitable for insulation where moisture resistance is critical. Graphene-cellulose aerogels leverage graphene's high conductivity and large surface area to achieve exceptional adsorption and electrochemical performance, but their mechanical brittleness may require further reinforcement. Polymer-cellulose aerogels offer excellent flexibility and biocompatibility, enabling uses in wearable sensors and drug carriers, though their thermal stability is often limited. Semiconductor-cellulose hybrids introduce photocatalytic activity, but their porosity must be optimized to ensure light penetration and reactant diffusion. Finally, MOF- or nanoparticle-loaded aerogels provide multifunctionality (e.g., antibacterial, sensing), yet the dispersion uniformity of the additives remains a challenge for scalable production.

Table 3: Performance comparison of nanocellulose-based hybrid aerogels.

Hybrid Aerogel Type	Key Components	Porosity/Density	Mechanical Properties	Functional Performance	Notable Applications	Ref.
Silica-cellulose	CNF, SiO_2	>95% porosity, ≈0.1 g/cm^3	Compressive modulus: 12.43 MPa; strength: 2.59 MPa	Thermal conductivity: 0.026–0.028 W/(m·K); moisture resistant	Thermal insulation, reinforced lightweight materials	[91,98]
Graphene-cellulose	CNF, GO/rGO	≈99% porosity, 3–15 mg/cm^3	Elastic recovery >90% after compression; anisotropic layered structure	Adsorption: 111.2 mg/g (methylene blue); conductivity: up to 11.78 S/cm; photothermal efficiency: 90.3%	Water purification, conductive scaffolds, photothermal devices	[92,99–101]
Polymer-cellulose	CNF, PVA/PPy/chitosan	High porosity (≈90%–98%), tunable pore geometry	Shape recovery >90%; flexible, compressible	Specific capacitance: 387.6 F/g; formaldehyde adsorption: 7.5 mmol/g; antibacterial activity	Supercapacitors, air filters, wound dressings	[93,106,107,117]
Semiconductor-cellulose	CNF, TiO_2/BiOBr	Hierarchical pores, high surface area	Moderate strength, often brittle	Photocatalytic dye degradation >90%; CO_2 conversion to $HCOOCH_3$ (yield 68.3%)	Photocatalysis, environmental remediation	[108–110,118]
MOF-/nanoparticle-cellulos	CNF, UiO-66/AgNPs	Porosity >95%, SSA up to 483 m^2/g	Compressive recovery >95% after 100 cycles	Antibacterial efficiency >99.9%; Hg^{2+} detection limit <1 ppm; stress-sensing capability	Gas adsorption, antibacterial materials, pressure sensors	[112,115,116]

This systematic comparison underscores that both the hybrid component and the nanocellulose source should be selected based on the desired application. For example, silica–CNF aerogels benefit from CNF's high aspect ratio and entanglement, yielding mechanically robust insulators, while silica–CNC composites may exhibit higher surface area but lower toughness. Similarly, graphene–CNF hybrids leverage CNF's fibrous network for elastic recovery, whereas graphene–CNC systems favor charge transport due to CNC's high crystallinity and dispersibility. Future research should focus on optimizing the synergy between nanocellulose and these additives to achieve balanced properties-e.g., high porosity with mechanical robustness, or high adsorption capacity with recyclability-while considering cost-effective and scalable fabrication routes.

4 Conclusion and Outlook

Cellulose aerogels have emerged as a potential class of materials with exceptional properties that make these attractive for a wide range of applications. Because of their high porosity, specific surface area, remarkable mechanical strength, and thermal stability, cellulose aerogels have demonstrated substantial potential in various fields including energy storage, thermal insulation, absorption, and biomedical engineering. Although significant progress has been made in the synthesis and characterization of cellulose

aerogels, further research is required to fully understand their properties and optimize their performance for specific applications. Herein, a combination of materials is integrated into cellulose aerogels. With continued advancements in this field, it is anticipated that cellulose aerogels will continue to play an increasingly important role in addressing the current societal challenges and facilitating sustainable development.

In conclusion, cellulose-based aerogels represent a rapidly advancing class of sustainable porous materials with immense potential across energy, environmental, and biomedical sectors. To fully realize this potential and enable their transition from laboratory to industry, future efforts must prioritize several interconnected challenges. First, advancing cost-effective and green fabrication protocols is essential, particularly through innovations in solvent systems and drying technologies to improve scalability and economic viability. Second, a deeper fundamental understanding of structure-property-performance relationships is needed to unlock their full capability in complex applications such as heterogeneous catalysis and sensing. Finally, reconciling the inherent trade-off between ultra-high porosity and mechanical robustness remains a central task. Innovative strategies in nanoscale engineering and hybrid material design will be key to developing aerogels that are both highly functional and sufficiently durable for practical use. Addressing these challenges will be pivotal in harnessing cellulose aerogels to meet pressing needs in sustainable technology and materials science.

Acknowledgement: We would like to express our special gratitude to the Education Department of Heilongjiang Province, the Mechanical Engineering College and the Sports College of Jiamusi University for their support.

Funding Statement: This research was funded by Basic Scientific Research Funds Project of Heilongjiang Universities of Department of Education, Heilongjiang Province, China, grant number 2025-KYYWF-ZR0763.

Author Contributions: Lin Jia: Data curation, writing—original draft, visualization, writing—review & editing. Qiang He: Visualization, writing—review & editing, supervision, funding. All authors reviewed and approved the final version of the manuscript.

Availability of Data and Materials: This study did not generate any new datasets. All data analyzed are from publicly available sources, as cited in the manuscript.

Ethics Approval: Not applicable.

Conflicts of Interest: The authors declare no conflicts of interest.

References

1. Mai T, Wang P-L, Ma M-G. Promising cellulose-based aerogel composites: preparation methods and advanced applications. Compos Part B Eng. 2024;281(1):111559. doi:10.1016/j.compositesb.2024.111559.
2. Alias BK, Peter S, Lyczko N, Nzihou A, Maria HJ, Thomas S. Cellulose nanofiber aerogel as a potential receiver layer for solar application: a review. Mater Today Sustain. 2023;24:100510. doi:10.1016/j.mtsust.2023.100510.
3. Zhao X, Chen L, Su PG, Xiao LX, Zhao HB, Fu T, et al. 4-Hydroxybenzenesulfonic acid triggers rapid preparation of phenolic aerogel composites by ambient pressure drying. Chem Eng J. 2024;479(43):147856. doi:10.1016/j.cej.2023.147856.
4. Wu C, Li K, Fei Z, Zhang Z, Zhao S, Chen G, et al. Preparation of high-performance SiO_2 aerogel using organic bases as catalysts and surfactants. Colloids Surf A Physicochem Eng Aspects. 2026;729(10):138950. doi:10.1016/j.colsurfa.2025.138950.
5. Lv S, Yuan Z, Zheng J, Liu Z, Ye J, Li J, et al. Preparation of reusable copper-based biomass-carbon aerogel catalysts and their application in highly selective reduction of maleimides to succinimides with hydrosilane as a hydrogen source. Green Chem. 2024;26(5):2592–8. doi:10.1039/d3gc04697d.

6. Chen D, Lee YY, Tan CP, Wang Y, Qiu C. Robust porous aerogel frameworks with high oil absorption derived from hierarchical nanocellulose/lipid nanoparticle composites. Carbohydr Polym. 2025;370(12):124442. doi:10.1016/j.carbpol.2025.124442.
7. Trembecka-Wojciga K, Lachowicz D, Terlicka S, Korneva A, Berent K, Sikora M, et al. Synergistic interactions of aerogel and liquid metal: a novel aerogel-reinforced metal matrix composite for advanced aerospace applications. Compos Part A Appl Sci Manuf. 2026;202:109525. doi:10.1016/j.compositesa.2025.109525.
8. Ghosh S, Yang CJ, Lai JY. Hollow nanoarchitectures: materials engineering, nanochemistry, and biomedical applications. Prog Mater Sci. 2026;158:101634. doi:10.1016/j.pmatsci.2025.101634.
9. Li Z, Li J, Guo J, Guan F, Zhang X, Yang Q, et al. Fabrication of multi-network aerogels based on *Sesbania* gum/nanocellulose and its application in oil recovery (from oily wastewater). Int J Biol Macromol. 2025;330:148226. doi:10.1016/j.ijbiomac.2025.148226.
10. Maleki H, Durães L, Portugal A. An overview on silica aerogels synthesis and different mechanical reinforcing strategies. J Non Cryst Solids. 2014;385:55–74. doi:10.1016/j.jnoncrysol.2013.10.017.
11. Liu W, Herrmann AK, Bigall NC, Rodriguez P, Wen D, Oezaslan M, et al. Noble metal aerogels—synthesis, characterization, and application as electrocatalysts. Acc Chem Res. 2015;48(2):154–62. doi:10.1021/ar500237c.
12. Kharissova OV, Ibarra Torres CE, González LT, Kharisov BI. All-carbon hybrid aerogels: synthesis, properties, and applications. Ind Eng Chem Res. 2019;58(36):16258–86. doi:10.1021/acs.iecr.9b03031.
13. Twej W. Temperature influence on the gelation process of tetraethylorthosilicate using sol-gel technique. Iraqi J Sci. 2009;50:43–9.
14. Hu X, Zhang S, Yang B, Hao M, Chen Z, Liu Y, et al. Preparation of ambient-dried multifunctional cellulose aerogel by freeze-linking technique. Chem Eng J. 2023;477(7844):147044. doi:10.1016/j.cej.2023.147044.
15. Halim ZAA, Awang N, Ahmad N, Yajid MAM. Effects of silane concentration on hydrophobic conversion of rice husk-derived silica aerogels prepared by supercritical drying. Biomass Convers Biorefin. 2024;14(14):15811–21. doi:10.1007/s13399-022-03710-8.
16. Jiang Z, Zhang X, Zhou G. Silica aerogels with tunable hydrophobicity for organic-water separation. Mater Chem Phys. 2026;349(2):131760. doi:10.1016/j.matchemphys.2025.131760.
17. Xie J, Niu L, Qiao Y, Lei Y, Li G, Zhang X, et al. The influence of the drying method on the microstructure and the compression behavior of graphene aerogel. Diam Relat Mater. 2022;121:108772. doi:10.1016/j.diamond.2021.108772.
18. Spiering GA, Godshall GF, Moore RB. Effect of the gel drying method on properties of semicrystalline aerogels prepared with different network morphologies. Gels. 2025;11(6):447. doi:10.3390/gels11060447.
19. Hou X, Kotsuka J, Sakuma W, Ito T, Kaku Y, Kobayashi Y, et al. Transparent insulators with a tough nanocellulose skeleton formed via freeze-drying. ACS Nano. 2026;20(4):3821–30. doi:10.1021/acsnano.5c19203.
20. Zhang XL, Jiang ZQ, Zhou GD. Synergistic *in situ* modification and solvent exchange for atmospheric drying of robust cellulose nanofiber aerogels toward organic compound/water separation. Mater Sci Eng B. 2026;324(2):119004. doi:10.1016/j.mseb.2025.119004.
21. Schneider R, Facure MHM, Chagas PAM, Andre RS, dos Santos DM, Correa DS. Tailoring the surface properties of micro/nanofibers using 0D, 1D, 2D, and 3D nanostructures: a review on post-modification methods. Adv Mater Interfaces. 2021;8(13):2100430. doi:10.1002/admi.202100430.
22. Hill R, Phipps J, Greenwood R, Skuse D, Zhang ZJ. The effect of pre-treatment and process conditions on the gas barrier properties of fibrillated cellulose films and coatings: a review. Carbohydr Polym. 2024;337:122085. doi:10.1016/j.carbpol.2024.122085.
23. Tang Z, Lin X, Yu M, Yang J, Li S, Mondal AK, et al. A review of cellulose-based catechol-containing functional materials for advanced applications. Int J Biol Macromol. 2024;266(Pt 2):131243. doi:10.1016/j.ijbiomac.2024.131243.
24. Qiu Y, Zhang C, Zhang M, Zheng D, Song D, Long S, et al. A feasible strategy of photothermal nanocellulose/chitosan porous composite with brine tolerance and magnetic controllability for solar-driven polluted seawater purification. Carbohydr Polym. 2025;369(6):124281. doi:10.1016/j.carbpol.2025.124281.
25. Yun T, Tao Y, Li Q, Cheng Y, Lu J, Lv Y, et al. Superhydrophobic modification of cellulosic paper-based materials: fabrication, properties, and versatile applications. Carbohydr Polym. 2023;305(11):120570. doi:10.1016/j.carbpol.2023.120570.

26. Heise K, Kontturi E, Allahverdiyeva Y, Tammelin T, Linder MB, Nonappa, et al. Nanocellulose: recent fundamental advances and emerging biological and biomimicking applications. Adv Mater. 2021;33(3):2004349. doi:10.1002/adma.202004349.
27. Aziz T, Farid A, Haq F, Kiran M, Ullah A, Zhang K, et al. A review on the modification of cellulose and its applications. Polymers. 2022;14(15):3206. doi:10.3390/polym14153206.
28. Wu C, Li J, Zhang YQ, Li X, Wang SY, Li DQ. Cellulose dissolution, modification, and the derived hydrogel: a review. ChemSusChem. 2023;16(21):e202300518. doi:10.1002/cssc.202300518.
29. Fatema N, Ceballos RM, Fan C. Modifications of cellulose-based biomaterials for biomedical applications. Front Bioeng Biotechnol. 2022;10:993711. doi:10.3389/fbioe.2022.993711.
30. Wang Y, Wang X, Xie Y, Zhang K. Functional nanomaterials through esterification of cellulose: a review of chemistry and application. Cellulose. 2018;25(7):3703–31. doi:10.1007/s10570-018-1830-3.
31. Beaumont M, Winklehner S, Veigel S, Mundigler N, Gindl-Altmutter W, Potthast A, et al. Wet esterification of never-dried cellulose: a simple process to surface-acetylated cellulose nanofibers. Green Chem. 2020;22(17):5605–9. doi:10.1039/d0gc02116d.
32. Tian W, Zhang J, Yu J, Wu J, Zhang J, He J, et al. Phototunable full-color emission of cellulose-based dynamic fluorescent materials. Adv Funct Mater. 2018;28(9):1703548. doi:10.1002/adfm.201703548.
33. Leszczyńska A, Radzik P, Szefer E, Mičušík M, Omastová M, Pielichowski K. Surface modification of cellulose nanocrystals with succinic anhydride. Polymers. 2019;11(5):866. doi:10.3390/polym11050866.
34. Nawaz H, Zhang J, Tian W, Jin K, Jia R, Yang T, et al. Cellulose-based fluorescent sensor for visual and versatile detection of amines and anions. J Hazard Mater. 2020;387:121719. doi:10.1016/j.jhazmat.2019.121719.
35. Jia R, Tian W, Bai H, Zhang J, Wang S, Zhang J. Amine-responsive cellulose-based ratiometric fluorescent materials for real-time and visual detection of shrimp and crab freshness. Nat Commun. 2019;10(1):795. doi:10.1038/s41467-019-08675-3.
36. Chen J, Zhou Z, Chen Z, Yuan W, Li M. A fluorescent nanoprobe based on cellulose nanocrystals with porphyrin pendants for selective quantitative trace detection of Hg^{2+}. New J Chem. 2017;41(18):10272–80. doi:10.1039/c7nj01263b.
37. Ciftci D, Ubeyitogullari A, Huerta RR, Ciftci ON, Flores RA, Saldaña MDA. Lupin hull cellulose nanofiber aerogel preparation by supercritical CO_2 and freeze drying. J Supercrit Fluids. 2017;127:137–45. doi:10.1016/j.supflu.2017.04.002.
38. Sun Y, Chu Y, Wu W, Xiao H. Nanocellulose-based lightweight porous materials: a review. Carbohydr Polym. 2021;255:117489. doi:10.1016/j.carbpol.2020.117489.
39. Wang Z, Yang X, Liu W. Structure control and application of nanocellulose aerogels. AATCC J Res. 2021;8(2_suppl):91–4. doi:10.14504/ajr.8.s2.18.
40. Filpponen I, Argyropoulos DS. Regular linking of cellulose nanocrystals via click chemistry: synthesis and formation of cellulose nanoplatelet gels. Biomacromolecules. 2010;11(4):1060–6. doi:10.1021/bm1000247.
41. Li B, Xu C, Liu L, Yu J, Fan Y. Facile and sustainable etherification of ethyl cellulose towards excellent UV blocking and fluorescence properties. Green Chem. 2021;23(1):479–89. doi:10.1039/d0gc02919j.
42. Sun L, Yang S, Qian X, An X. High-efficacy and long term antibacterial cellulose material: anchored guanidine polymer via double click chemistry. Cellulose. 2020;27(15):8799–812. doi:10.1007/s10570-020-03374-5.
43. Zhang T, Zhang Y, Wang X, Liu S, Yao Y. Characterization of the nano-cellulose aerogel from mixing CNF and CNC with different ratio. Mater Lett. 2018;229:103–6. doi:10.1016/j.matlet.2018.06.101.
44. Wu Z, Zhang T, Zhang H, Liu R, Chi H, Li X, et al. One-pot fabrication of hydrophilic-oleophobic cellulose nanofiber-silane composite aerogels for selectively absorbing water from oil-water mixtures. Cellulose. 2021;28(3):1443–53. doi:10.1007/s10570-020-03610-y.
45. Neves RM, Ornaghi HL Jr, Zattera AJ, Amico SC. The influence of silane surface modification on microcrystalline cellulose characteristics. Carbohydr Polym. 2020;230(1):115595. doi:10.1016/j.carbpol.2019.115595.
46. Redl FX, Lutz M, Daub J. Chemistry of porphyrin-appended cellulose strands with a helical structure: spectroscopy, electrochemistry, and *in situ* circular dichroism spectroelectrochemistry. Chemistry. 2001;7(24):5350–8. doi:10.1002/1521-3765(20011217)7:.

47. Ruello JLA, Mujmule RB, Kassahun SK, Kiflie Z, Kim H. Production of superhydrophobic cardboard-based aerogel for effective oil recovery. Sustain Mater Technol. 2025;44:e01340. doi:10.1016/j.susmat.2025.e01340.
48. Wang Y, Huang JX, Guo ZG. Coir fiber-reinforced PVA aerogels for oil adsorption. New J Chem. 2022;46(34):16265–8. doi:10.1039/d2nj02583c.
49. Sousa Pereira AL, Feitosa JPA, Saraiva Morais JP, de Freitas Rosa M. Cellulose source tailors the physical and structural properties of double-functionalized aerogels. J Nat Fibres. 2023;20(1):2140377. doi:10.1080/15440478.2022.2140377.
50. Meng T, Gao X, Zhang J, Yuan J, Zhang Y, He J. Graft copolymers prepared by atom transfer radical polymerization (ATRP) from cellulose. Polymer. 2009;50(2):447–54. doi:10.1016/j.polymer.2008.11.011.
51. Chu Y, Huang Z, Liang K, Guo J, Boyer C, Xu J. A photocatalyst immobilized on fibrous and porous monolithic cellulose for heterogeneous catalysis of controlled radical polymerization. Polym Chem. 2018;9(13):1666–73. doi:10.1039/c7py01690e.
52. Barsbay M, Güven O. Surface modification of cellulose via conventional and controlled radiation-induced grafting. Radiat Phys Chem. 2019;160:1–8. doi:10.1016/j.radphyschem.2019.03.002.
53. Rajan STK, Nagarajan KJ, Balasubramani V, Sathickbasha K, Sanjay MR, Siengchin S, et al. Investigation of mechanical and thermo-mechanical characteristics of silane-treated cellulose nanofibers from agricultural waste reinforced epoxy adhesive composites. Int J Adhes Adhes. 2023;126(3):103492. doi:10.1016/j.ijadhadh.2023.103492.
54. Zhu W, Ji M, Zhang Y, Wang Z, Chen W, Xue Y. Synthesis and characterization of aminosilane grafted cellulose nanocrystal modified formaldehyde-free decorative paper and its CO_2 adsorption capacity. Polymers. 2019;11(12):2021. doi:10.3390/polym11122021.
55. Yang Q, Pan X. A facile approach for fabricating fluorescent cellulose. J Appl Polym Sci. 2010;117(6):3639–44. doi:10.1002/app.32287.
56. Lucia A, Bacher M, van Herwijnen HWG, Rosenau T. A direct silanization protocol for dialdehyde cellulose. Molecules. 2020;25(10):2458. doi:10.3390/molecules25102458.
57. Araki J, Wada M, Kuga S. Steric stabilization of a cellulose microcrystal suspension by poly(ethylene glycol) grafting. Langmuir. 2001;17(1):21–7. doi:10.1021/la001070m.
58. Kuga S, Wu M. Mechanochemistry of cellulose. Cellulose. 2019;26(1):215–25. doi:10.1007/s10570-018-2197-1.
59. Lin W, Wu S, Han S, Xie J, He H, Zou Q, et al. Preparation and characterization of highly conductive lignin aerogel based on tunicate nanocellulose framework. Int J Biol Macromol. 2023;242(12):125010. doi:10.1016/j.ijbiomac.2023.125010.
60. Zhu Y, Li H, Huang W, Lai X, Zeng X. Facile fabrication of superhydrophobic wood aerogel by vapor deposition method for oil-water separation. Surf Interfaces. 2023;37:102746. doi:10.1016/j.surfin.2023.102746.
61. Khattab TA, Dacrory S, Abou-Yousef H, Kamel S. Development of microporous cellulose-based smart xerogel reversible sensor via freeze drying for naked-eye detection of ammonia gas. Carbohydr Polym. 2019;210(21):196–203. doi:10.1016/j.carbpol.2019.01.067.
62. Lee KY, Aitomäki Y, Berglund LA, Oksman K, Bismarck A. On the use of nanocellulose as reinforcement in polymer matrix composites. Compos Sci Technol. 2014;105:15–27. doi:10.1016/j.compscitech.2014.08.032.
63. Qu G, Wei Y, Zhao L, Liu J, Liu X, He H, et al. Physical modifications of cellulose nanocrystals by poly(d-lactic acid) and poly(ethylene glycol) (PDLA-PEG-PDLA) block copolymer to improve the mechanical properties of polylactide. Polymer. 2024;292:126609. doi:10.1016/j.polymer.2023.126609.
64. Arumughan V, Nypelö T, Hasani M, Larsson A. Fundamental aspects of the non-covalent modification of cellulose via polymer adsorption. Adv Colloid Interface Sci. 2021;298(7):102529. doi:10.1016/j.cis.2021.102529.
65. Xia T, Huang Y, Lan P, Lan L, Lin N. Physical modification of cellulose nanocrystals with a synthesized triblock copolymer and rheological thickening in silicone oil/grease. Biomacromolecules. 2019;20(12):4457–65. doi:10.1021/acs.biomac.9b01186.
66. Sun Z, Ni Y, Prakasam T, Liu W, Wu H, Zhang Z, et al. The unusual photochromic and hydrochromic switching behavior of cellulose-embedded 1,8-naphthalimide-viologen derivatives in the solid-state. Chemistry. 2021;27(36):9360–71. doi:10.1002/chem.202100601.

67. Wendler F, Kosan B, Krieg M, Meister F. Possibilities for the physical modification of cellulose shapes using ionic liquids. Macromol Symp. 2009;280(1):112–22. doi:10.1002/masy.200950613.
68. Zhou J, Hsieh YL. Conductive polymer protonated nanocellulose aerogels for tunable and linearly responsive strain sensors. ACS Appl Mater Interfaces. 2018;10(33):27902–10. doi:10.1021/acsami.8b10239.
69. Liu G, Li J, Li X, Pan X, Qian C. Preparation and properties of novel superhydrophobic cellulose nanofiber aerogels. J Nanomater. 2021;2021:2631405. doi:10.1155/2021/2631405.
70. Ke W, Ge F, Shi X, Zhang Y, Wu T, Zhu X, et al. Superelastic and superflexible cellulose aerogels for thermal insulation and oil/water separation. Int J Biol Macromol. 2024;260(5):129245. doi:10.1016/j.ijbiomac.2024.129245.
71. Zhang F, Wang C, Zhou J, Wu J, Gu H, Lin W. Hydrophobic sponge derived from natural loofah for efficient oil/water separation. Sep Purif Technol. 2024;330:125519. doi:10.1016/j.seppur.2023.125519.
72. Xu X, Zou J, Xiao Z, Zhang J, Wang B, Jiang J, et al. Crystalline ZnO aerogel microspheres for boosting photocatalytic CO_2 reduction. Fuel. 2025;398:135519. doi:10.1016/j.fuel.2025.135519.
73. Kim CH, Youn HJ, Lee HL. Preparation of surface-charged CNF aerogels and investigation of their ion adsorption properties. Cellulose. 2017;24(7):2895–902. doi:10.1007/s10570-017-1321-y.
74. Wei J, Yang S, Zhu Z, Lu J, Zhang B, Zhang M, et al. Low-temperature dried alginate/silica hybrid aerogel beads with tunable surface functionalities for removal of lead ions from water. Gels. 2025;11(6):397. doi:10.3390/gels11060397.
75. An J, Ping X, Gao G, Shen Q, Wang Z, Zhang C, et al. High flame-retardant and thermal insulation performances of sodium-alginate/chitosan aerogel by coating montmorillonite on pore surface. Ceram Int. 2025;51(25):45510–21. doi:10.1016/j.ceramint.2025.07.268.
76. Zong D, Cao L, Sun Y, Pang S, Li Y, Liu Y. Fast, low-cost, and lyophilization-free synthesis of multifunctional elastic nanofiber aerogels. Small. 2025;21(25):e2412778. doi:10.1002/smll.202412778.
77. Tong Y, Xue F, Lu X, Liao X, Meng J, Zhong L, et al. Bacterial cellulose carbon aerogel with ultra-high stress retention for flexible sensor. Int J Biol Macromol. 2025;320:145681. doi:10.1016/j.ijbiomac.2025.145681.
78. Shen J, Hou S, Li C, Yin K, Zhong L, Bi H, et al. Bidirectional phase separation spinning under natural drying to prepare aerogel fibers for thermal insulation. Adv Sci. 2025;12(34):e05306. doi:10.1002/advs.202505306.
79. Lee H, Song J, Park CB, Lee S, Jang JD, Koo J. Enhanced properties of silica aerogels/melt-blown nonwoven composites: a comparative study of supercritical CO_2 and freeze-drying methods. J Mater Sci. 2025;60(30):12747–65. doi:10.1007/s10853-025-11162-4.
80. Hu X, Li H, Tong C, Yang S, Li Y, Zhu R, et al. Effect of solvent exchange on silica aerogel properties via ambient pressure drying. J Sol Gel Sci Technol. 2025;116(2):972–82. doi:10.1007/s10971-025-06831-4.
81. Zhuo C, Bo Y, Liu Q, Xu S, Qu H, Chen X, et al. Tough and thermal insulated poly(phthalazinone ether sulfone ketone) aerogel fibers fabricated via ambient pressure drying. ACS Appl Polym Mater. 2025;7(20):13661–72. doi:10.1021/acsapm.5c02482.s001.
82. Jiang W, Zhao Y, Wang W, Zeng Q, Li H, Zeng X, et al. Ambient-pressure dried multifunctional silicone/MXene composite aerogel for smart fire protection. Compos Part A Appl Sci Manuf. 2025;198(1):109106. doi:10.1016/j.compositesa.2025.109106.
83. Al Abdallah H, Tannous JH, Abu-Jdayil B. Cellulose and nanocellulose aerogels, their preparation methods, and potential applications: a review. Cellulose. 2024;31(4):2001–29. doi:10.1007/s10570-024-05743-w.
84. Valencia L, Abdelhamid HN. Nanocellulose leaf-like zeolitic imidazolate framework (ZIF-L) foams for selective capture of carbon dioxide. Carbohydr Polym. 2019;213(3):338–45. doi:10.1016/j.carbpol.2019.03.011.
85. Wang L, Xu H, Gao J, Yao J, Zhang Q. Recent progress in metal-organic frameworks-based hydrogels and aerogels and their applications. Coord Chem Rev. 2019;398:213016. doi:10.1016/j.ccr.2019.213016.
86. Lin F, Wang Z, Shen Y, Tang L, Zhang P, Wang Y, et al. Natural skin-inspired versatile cellulose biomimetic hydrogels. J Mater Chem A. 2019;7(46):26442–55. doi:10.1039/c9ta10502f.
87. Prasad C, Jeong SG, Won JS, Ramanjaneyulu S, Sangaraju S, Kerru N, et al. Review on recent advances in cellulose nanofibril based hybrid aerogels: synthesis, properties and their applications. Int J Biol Macromol. 2024;261:129460. doi:10.1016/j.ijbiomac.2024.129460.

88. Abraham E, Cherpak V, Senyuk B, ten Hove JB, Lee T, Liu Q, et al. Highly transparent silanized cellulose aerogels for boosting energy efficiency of glazing in buildings. Nat Energy. 2023;8(4):381–96. doi:10.1038/s41560-023-01226-7.
89. Zhao Y, Zeng Q, Lai X, Li H, Zhao Y, Li K, et al. Multifunctional cellulose-based aerogel for intelligent fire fighting. Carbohydr Polym. 2023;316:121060. doi:10.1016/j.carbpol.2023.121060.
90. Revin VV, Nazarova NB, Tsareva EE, Liyaskina EV, Revin VD, Pestov NA. Production of bacterial cellulose aerogels with improved physico-mechanical properties and antibacterial effect. Front Bioeng Biotechnol. 2020;8:603407. doi:10.3389/fbioe.2020.603407.
91. Fu J, Wang S, He C, Lu Z, Huang J, Chen Z. Facilitated fabrication of high strength silica aerogels using cellulose nanofibrils as scaffold. Carbohydr Polym. 2016;147(5):89–96. doi:10.1016/j.carbpol.2016.03.048.
92. Wang M, Shao C, Zhou S, Yang J, Xu F. Super-compressible, fatigue resistant and anisotropic carbon aerogels for piezoresistive sensors. Cellulose. 2018;25(12):7329–40. doi:10.1007/s10570-018-2080-0.
93. Zhuo H, Hu Y, Chen Z, Zhong L. Cellulose carbon aerogel/PPy composites for high-performance supercapacitor. Carbohydr Polym. 2019;215:322–9. doi:10.1016/j.carbpol.2019.03.101.
94. Zhang H, Jiang T, He X, Chen T, Fan L, Gao M, et al. Preparation and properties of cellulose nanofibril-graphene nanosheets/polyaniline composite conductive aerogels. BioResources. 2020;15(1):1828–43. doi:10.15376/biores.15.1.1828-1843.
95. Gu H, Zhou X, Lyu S, Pan D, Dong M, Wu S, et al. Magnetic nanocellulose-magnetite aerogel for easy oil adsorption. J Colloid Interface Sci. 2020;560:849–56. doi:10.1016/j.jcis.2019.10.084.
96. Zhuo X, Liu C, Pan R, Dong X, Li Y. Nanocellulose mechanically isolated from *Amorpha fruticosa* Linn. ACS Sustain Chem Eng. 2017;5(5):4414–20. doi:10.1021/acssuschemeng.7b00478.
97. Uddin KMA, Orelma H, Mohammadi P, Borghei M, Laine J, Linder M, et al. Retention of lysozyme activity by physical immobilization in nanocellulose aerogels and antibacterial effects. Cellulose. 2017;24(7):2837–48. doi:10.1007/s10570-017-1311-0.
98. Demilecamps A, Beauger C, Hildenbrand C, Rigacci A, Budtova T. Cellulose-silica aerogels. Carbohydr Polym. 2015;122:293–300. doi:10.1016/j.carbpol.2015.01.022.
99. Wang Z, Song L, Wang Y, Zhang XF, Yao J. Construction of a hybrid graphene oxide/nanofibrillated cellulose aerogel used for the efficient removal of methylene blue and tetracycline. J Phys Chem Solids. 2021;150:109839. doi:10.1016/j.jpcs.2020.109839.
100. Wu G, Bing N, Li Y, Xie H, Yu W. Three-dimensional directional cellulose-based carbon aerogels composite phase change materials with enhanced broadband absorption for light-thermal-electric conversion. Energy Convers Manag. 2022;256:115361. doi:10.1016/j.enconman.2022.115361.
101. Yao Q, Fan B, Xiong Y, Jin C, Sun Q, Sheng C. 3D assembly based on 2D structure of cellulose nanofibril/graphene oxide hybrid aerogel for adsorptive removal of antibiotics in water. Sci Rep. 2017;7(1):45914. doi:10.1038/srep45914.
102. Wu L, Gao L, Li J, Wu T, Chen D, Zhou M, et al. Ultralight, super-compression, and hydrophobic nanofibrous aerogels from cellulose acetate/polyethylene oxide nanofibers for efficient and recyclable oil absorption. New J Chem. 2023;47(16):7930–8. doi:10.1039/d3nj00521f.
103. Chen Y, Yu Z, Han Y, Yang S, Fan D, Li G, et al. Combination of water-soluble chemical grafting and gradient freezing to fabricate elasticity-enhanced and anisotropic nanocellulose aerogels. Appl Nanosci. 2020;10(2):411–9. doi:10.1007/s13204-019-01162-7.
104. Zhao Y, Li B, Zhong M, Fan H, Li Z, Lyu S, et al. Highly sensitive, wearable piezoresistive methylcellulose/chitosan@MXene aerogel sensor array for real-time monitoring of physiological signals of pilots. Sci China Mater. 2025;68(2):542–51. doi:10.1007/s40843-024-3188-4.
105. Li H, Li X, Quan F, Chen Z, Xia Y, Xiong Z. Wide-spectrum dye adsorption performance of alginic acid carbon aerogel. Water Air Soil Pollut. 2024;235(6):375. doi:10.1007/s11270-024-07181-7.
106. Liao Y, Pan X. Self-indicating and high-capacity mesoporous aerogel-based biosorbent fabricated from cellulose and chitosan via co-dissolution and regeneration for removing formaldehyde from indoor air. Environ Sci Nano. 2021;8(5):1283–95. doi:10.1039/d1en00122a.

107. Zhang L, Liao Y, Wang YC, Zhang S, Yang W, Pan X, et al. Cellulose II aerogel-based triboelectric nanogenerator. Adv Funct Mater. 2020;30(28):2001763. doi:10.1002/adfm.202001763.
108. Zhou W, Sun S, Jiang Y, Zhang M, Lawan I, Fernando GF, et al. Template *in situ* synthesis of flower-like BiOBr/microcrystalline cellulose composites with highly visible-light photocatalytic activity. Cellulose. 2019;26(18):9529–41. doi:10.1007/s10570-019-02722-4.
109. Zhou W, Ye H, Zhong Z, Lu Q, Liu R, Zhang M, et al. Modification of BiOBr with cellulose nanocrystals to improve the photocatalytic performance under visible light. Cellulose. 2021;28(15):9893–905. doi:10.1007/s10570-021-04153-6.
110. Maimaiti H, Awati A, Yisilamu G, Zhang D, Wang S. Synthesis and visible-light photocatalytic CO_2/H_2O reduction to methyl formate of TiO_2 nanoparticles coated by aminated cellulose. Appl Surf Sci. 2019;466:535–44. doi:10.1016/j.apsusc.2018.10.070.
111. Cho K, Andrew LJ, MacLachlan MJ. Uniform growth of nanocrystalline ZIF-8 on cellulose nanocrystals: useful template for microporous organic polymers. Angew Chem Int Ed. 2023;62(24):e202300960. doi:10.1002/anie.202300960.
112. Seo JY, Song Y, Lee JH, Kim H, Cho S, Baek KY. Robust nanocellulose/metal-organic framework aerogel composites: superior performance for static and continuous disposal of chemical warfare agent simulants. ACS Appl Mater Interfaces. 2021;13(28):33516–23. doi:10.1021/acsami.1c08138.
113. Zou Y, Zhao J, Zhu J, Guo X, Chen P, Duan G, et al. A mussel-inspired polydopamine-filled cellulose aerogel for solar-enabled water remediation. ACS Appl Mater Interfaces. 2021;13(6):7617–24. doi:10.1021/acsami.0c22584.
114. Shi Z, Gao H, Feng J, Ding B, Cao X, Kuga S, et al. *In situ* synthesis of robust conductive cellulose/polypyrrole composite aerogels and their potential application in nerve regeneration. Angew Chem Int Ed. 2014;53(21):5380–4. doi:10.1002/anie.201402751.
115. Yao Q, Fan B, Xiong Y, Wang C, Wang H, Jin C, et al. Stress sensitive electricity based on Ag/cellulose nanofiber aerogel for self-reporting. Carbohydr Polym. 2017;168(11):265–73. doi:10.1016/j.carbpol.2017.03.089.
116. Matsuyama K, Morotomi K, Inoue S, Nakashima M, Nakashima H, Okuyama T, et al. Antibacterial and antifungal properties of Ag nanoparticle-loaded cellulose nanofiber aerogels prepared by supercritical CO_2 drying. J Supercrit Fluids. 2019;143:1–7. doi:10.1016/j.supflu.2018.08.008.
117. Wang J, Xu J, Zhu S, Wu Q, Li J, Gao Y, et al. Preparation of nanocellulose in high yield via chemi-mechanical synergy. Carbohydr Polym. 2021;251(3):117094. doi:10.1016/j.carbpol.2020.117094.
118. Kettunen M, Silvennoinen RJ, Houbenov N, Nykänen A, Ruokolainen J, Sainio J, et al. Photoswitchable superabsorbency based on nanocellulose aerogels. Adv Funct Mater. 2011;21(3):510–7. doi:10.1002/adfm.201001431.